Title	TIME RESOLVED STUDIES ON DYNAMIC BEHAVIOUR OF ATOMIC AND IONIC SPECIES AND ON LASER ACTIONS IN CONDENSED DISCHARGE ARGON PLASMAS
Author(s)	Koda, Toshio
Citation	大阪大学, 1974, 博士論文
Version Type	VoR
URL	https://hdl.handle.net/11094/2530
rights	
Note	

TIME RESOLVED STUDIES ON DYNAMIC BEHAVIOUR OF ATOMIC AND IONIC SPECIES AND ON LASER ACTIONS IN CONDENSED DISCHARGE ARGON PLASMAS

by

Toshio KODA

Submitted to Graduate School of Science in Partial Fulfilment

of the Requirements for the Degree of

Doctor of Science

OSAKA UNIVERSITY

1974

CONTENTS

Abstract

In Part I, time resolved studies have been carried out on dynamic behaviour of atomic and ionic species in condensed discharge argon plasmas. A spectroscopic two-channel-streak-camera, which has been newly designed and constructed for the purpose of studying the breakdown in condensed discharges of various types, enables one to trace quick motions of different kinds of emitting species, simultaneously. In addition, this camera with some modification is applicable to condensed discharge plasmas for time resolved studies of the line broadening. After its applications to the hot plasmas of a linear pinch, a tubular pinch, and a wire explosion caused by condensed discharges, it has been proved that the camera constructed is of good use for high temperature plasma diagnostics. Especially, it enables one to see how different kinds of species existent in a hot plasma behave in different manners of their own.

Time resolved studies on laser actions have been carried out in Part II. An extremely high current pulsed discharge tube filled with argon, which is 5 mm in diameter and 140 cm in length, gives four laser lines at the wavelengths of 4880, 4765, 3638 and 3511 Å. Time resolved studies have been carried out on the

pressure effect, the voltage effect, the impurity effect and the high frequency field effect of these lines. Two different laser pulse modes have been confirmed. The primary laser pulse composed of the line 4765 of ArII, the lines 3511 and 3638 of ArIII, occurs at the early stage of the discharge. On the other hand, the secondary laser pulse, which consists only of the line 4880 of ArII, takes place in the afterglow of the discharge. For explanation of all the experimental results obtained, an excitation mechanism for the line 4880 have been newly proposed. In addition, argon ion laser actions have been realized in such a plasma as produced by a linear pinch discharge. The present observation shows that there are no correlations between laser actions and pinch phenomena, as long as the periods of the linear pinch discharge currents are about 30 μsec. Laser actions take place only at the beginning of the discharge in spite of its long period.

PART I

TIME RESOLVED STUDIES ON DYNAMIC BEHAVIOUR OF ATOMIC AND IONIC SPECIES

(1) Introduction

High temperature plasmas are often produced in various ways by means of condensed discharges. They usually fall into decay soon after transient processes of very short durations. There are commonly several kinds of ionic and neutral species in such a short-lived plasma as produced in laboratory. Occasionally, it seems to be inevitable that even impurity ions are present within such a discharge plasma. Each kind of species has its own mass, charge, and other physical properties. In addition, condensed discharges are generally poor in reproducibility, to be exact. Accordingly, it may be most desirable to trace quick motions of different kinds of emitting species simultaneously, in order to see how they behave in different manners, or how they are in cooperation with each other, throughout a transitory life of a high temperature plasma.

For that purpose, a spectroscopic two-channel-streak-camera was made for trial. Part I is the first report about its instrumentation and some information obtained through its appications to the condensed discharge argon plasma.

(2) Spectroscopic Two-Channel-Streak-Camera

The spectroscopic two-channel-streak-camera is composed of three parts; an anastigmatic spectrograph with a plane grating and two achromatic lenses, a streak camera with a double-hexagonal rotating mirror, and a reflector cabinet inserted between the two above. The spectrograph is fitted with two exit slits in place of a plate holder. Any two picked out of all the spectral lines emerging from a transitory plasma are admitted through the two exit slits, whose images are both brought into focus on separate films set in the interior of the streak camera with the aid of the reflector cabinet. An outside view of the whole, which is $50 \times 65 \times 120$ cm in size, is shown in Fig.1.

The anastigmatic spectrograph consists of a collimator lens with an aperture of 60 mm and a focal distance of 100 mm, a plane grating with a ruled surface of 65×75 mm, a ruling of 1200 grooves per mm and a blaze at 3000Å, and a camera lens with an aperture of 50 mm and a focal distance of 100 mm. The lenses are both achromatic over the wavelength range 2000 to 8000Å. Each of the lenses is a combination of three pieces made of fused quartz and LiF. In order that observations of transient phenomena may be aimed at, the F-number of the spectrograph should be as low as possible, while the dispersion should not be reduced too much. The present spectrograph is designed for the F-number of 4, the inverse dispersion of 40Å/mm, and the resolving power of 6×10^4 in the first order spectrum.

An image of a transitory plasma is formed by a couple of concave mirrors on the inlet slit of the spectrograph. A lot of anastigmatic and monochromatic images of the inlet slit are lined up on the focal plane of the camera lens. It is possible to move horizontally along the focal plane the two exit slits, whose positions and widths are adjustable separately. One of the exit slits allows a monochromatic radiation from a kind of emitting species to pass through, while the other admits another monochromatic radiation emitted by a different kind of species. For instance, when a condensed discharge takes place through argon, the neutral and singly ionized argon can be chosen as two different species. If necessary, a limited wavelength range of continuum and a spectral line emitted by an impurity ion can be selected as a pair by the two exit slits.

After passing through one of the exit slits, a monochromatic radiation is brought into focus on one of the films (35 mm in width) mounted in the inside of the spectroscopic two-channel-streak-camera by means of the reflector cabinet and a pair of lenses, as illustrated in Fig.2. The cabinet has six plane mirrors in it, where small screws interlock the exit slits and the mirrors. A set of three mirrors within the cabinet and a couple of lenses in front of the rotating mirror convert a vertical line of monochromatic image at the exit slit into a horizontal one, which is perpendicular to the direction of sweep on the film. Focussing on the film is achieved by adjusting the separation of the doublet along the optical axis.

The streak camera is nearly the same as the conventional one, except for the double-hexagonal rotating mirror, which is cut out of one block of stainless steel. The twelve surfaces of reflection are polished optically flat and coated with aluminum. The double-hexagonal mirror can rotate without damage at the highest speed of 2×10^4 revolutions per minute. The maximum speed corresponds to the sweep velocity of 0.7 mm/μsec on the film. The rotating mirror is driven by an a.c. motor, the r.p.s. of which is nearly proportional to the input voltage.

(3) Simultaneous Tracings of Motions of Atomic and Ionic Species

There have already been several experimental studies on the phenomena of condensed discharges by means of a conventional streak camera[1)], a framing camera[2)], and others[3)]. Those experiments, however, have not yet given any direct information about individual behaviour of different species taking part in condensed discharges. The subject of this section is to see through the present camera whether any two different kinds of emitting species behave in the same manner or not.

a) NaI and ArII in linear pinch

The discharge chamber used is a soft glass cylinder of 10 cm in inner diameter and 50 cm in length with ends closed by stainless steel plates. One of the plates is connected to a condenser bank of 100 μF through a vacuum switch, and the other is grounded through six thin copper belts which surround the glass cylinder concentrically and serve as return circuits. The chamber is evacuated by an oil diffusion pump down to about 1×10^{-5} torr and then argon gas is admitted at the pressure of one torr. Discharge is forced at the applied voltage of 10 kV.

The cross-section of the discharge tube at the central portion in the length is focussed on the slit of the F:4 spectrograph which is a part of the present streak camera. An example of time-integrated spectrum obtained is shown in Fig.3. The emission spectrum consists of strong ArII lines, weak ArI lines, intensive impurity lines and a continuum. Relative intensities of these lines depend upon initial pressures and voltages.

To begin with, let the two spectral lines; NaI 5893Å and ArII 4880Å, be admitted into the two-channel-streak-camera, a typical photo as shown in Fig.4 is obtained under the condition of one torr and 10 kV. Generally speaking[1),4)], the process of contraction and expansion is repeated several times during one discharge period in both of the streak patterns. When the discharge takes place, a luminous sheet caused by a high current starts from the wall and is contracted towards the axis of the tube to form the first pinch. This initial pinch is followed by the second pinch through an expansion period. Such repeated processes give rise to the third pinch and so on. Each period of the repetition becomes longer, but no difference is observed between the two species selected.

However, different emitters really show different behaviour when the patterns are examined in some detail. As seen in Fig.4, the NaI emission has a longer life than the ArII emission. After the initial pinch, the ArII streak pattern shows a strong emission when a contraction occurs, i.e. at the pinch time. On the other hand, a strong emission is observed in the NaI pattern when an expansion sheet is reflected at the wall as well as at the pinch time. At the same time, a pinch phenomenon is considerablly suppressed in the NaI pattern in progression; for instance, the third pinch is not clearly observed in comparison with the ArII pattern, and finally the NaI emission covers the whole discharge region after the argon ion emission disappears.

These facts suggest that the collision of an expansion sheet with the wall causes evaporation and excitation of sodium atoms which are contained in the soft glass wall. Since neutral atoms have no motive force to contract by themselves, the pinch becomes indistinct in successive periods even though NaI emission is observed. In addition, the NaI pattern shows some heterogeneous character in emission. That is to say, many narrow stripes of emission are observed after the initial pinch. It might be a reflection of inhomogeneous conditions of the wall surface.

The ArII pattern does not show such stripes of emission, but does a conical zone of bright emission just after the second, third and fourth pinches. If it is assumed that contractions with various speeds are formed through a reflection of the preceding expansion sheet at the wall, a part of argon ions with fast speed reaches the pinch and during its next expansion period it meets another part with slow speeds. As a result, the conical zone of bright emission may be formed after the pinch. In fact, the formation of contraction sheets with various speeds is observed after the first reflection of expansion sheet at the wall. Such a behaviour is not clearly observed at the third or fourth pinch perhaps because of weak emissions. In the NaI pattern the conical zone of emission is also observed, but not clearly partly because of an interference of many stripes of emission.

b) SiII and ArII in linear pinch

In the next place, let the two spectral lines; SiII 4128Å and ArII 4880Å; be introduced into the two-channel-streak-camera, a typical photo as shown in Fig.5 is obtained under the same condition as above. An increase in the sweep velocity leads to an increase of time resolution at the expense of the photographic density as seen in Fig.5. This is one of the reasons why the ArII pattern in this figure differs apparently from that in Fig.4 in spite of the same condition of discharge. Another reason may be due to poor reproducibility of the condensed discharge.

At any rate, the SiII pattern is quite different from the ArII pattern. The former exhibits a well defined luminous region during the expansion period following the initial pinch. The SiII pattern shows another contraction sheet starting at the initial pinch. When this contraction sheet meets the expansion sheet following the first pinch, such a bright emission comes out with a short duration. Many narrow stripes of emission are observed in the SiII pattern, too. These stripes might be related to the surface condition, being similar to those observed in the NaI pattern.

It is noted here that an emission over the whole discharge region is observed at the initial pinch in all the patterns observed. In the present setup of the optical system, these streak patterns do not represent the true distribution of light intensity over the discharge space directly, because the light falling onto a certain part of the slit is a sum of emission along the corresponding optical path. If assumed that the plasma is cylindrically symmetric, the radial distribution of light intensity can be obtained by means of the so-called Abel transformation from the intensity distribution on the film. An example of the results obtained in such a way is shown in Fig.6 for the case of the SiII pattern at the initial pinch. Fig.6 tells us that a strong emission is caused by the initial pinch near the axis of the tube and that another emission, although being weak, appears close by the wall surface. Moreover, the weak emission near the wall is observed in every one of the patterns obtained, irrespective of emitting species available. Judging from these facts, this emission may not be a line spectrum coming from a particular species but a continuum or fluoresence from the glass surface. Ultraviolet radiation[5], or shock wave with very high speed accompanied by the initial pinch may give rise to such an emission at the wall.

c) ArI and ArII in tubular pinch

As is well known[2),6)], a tubular pinch device is a discharge tube where a plasma is pinched into a cylindrical sheet between two coaxial copper cylinders, each of which carries a part of the return current. Since the device used here has previously been reported in detail[7], only a few dimensions are cited as follows. The discharge space is limited by two insulating tubes, where the outer glass tube is 18 cm in diameter and 40 cm in length, and the inner quartz tube is 9 cm in diameter and 40 cm in length. Both ends of them are enclosed by terminal copper plates. The capacitance of a condenser bank is 50 μF and the applied voltage up to 20 kV.

The light coming through a quartz window attached to the copper plate is focussed onto the slit of the spectrograph.

The direction of sight is parallel to the axis of the tube, and so the middle portion of the tube in the length can be observed immediately. When the initial pressure is raised, ArI lines become stronger and ArII lines weaker. The pinch phenomena are well observed at lower pressures[7]. Some examples of the streak patterns obtained are displayed in Fig.7, where the two spectral lines selected are ArII 4880Å and ArI 4300Å.

The three pairs of patterns show a pressure dependence of the mechanism of the so-called tubular pinch. Intensities of the ArI and ArII lines increase rapidly towards the initial pinch at the pressure of 1 torr. On the contrary, emissions of both lines are suppressed towards the initial pinch and finally disappear at the pressure of 5 torr. At the pressure of 3 torr, the ArII line decreases in intensity for a while on the way of the initial pinch in contrast to the ArI line, which increases monotonously in intensity.

It may be worth-while to notice here that a satellite pinch pattern can be seen just behind the main current sheet. It must be due to a secondary current sheet. However, such a satellite pattern can not be recognized at the pressure of 1 torr, but it is greatly enhanced by increasing pressures 3 to 5 torr. Accordingly,

Fig.7 suggests that systematic studies with a variety of initial pressures and voltages may enable one to have much better understanding of the tubular pinch mechanism by the use of atomic and ionic lines.

d) H_β and ArII in tubular pinch

When a mixture of argon and water vapor is used as a filling gas in tubular pinch device, intense lines of H_β, H_γ and H_δ are emitted as well as argon lines, as shown in Fig.8. The figure also shows that H_β is well isolated from a number of strong lines emitted by ArII. Then the pair of the H_β 4861Å and ArII 4379Å lines can be introduced into the two-channel-streak-camera. As shown in Fig.9, the H_β pattern continues for much longer duration than the ArII pattern does. The ArII pattern shows only the first and second pinches during single discharge period. The H_β pattern, however, shows several pinches, although the pinch becomes obscure one after another. Finally, it becomes diffuse completely for a long duration. Such a behaviour is similar to the NaI pattern in the linear pinch discharge as mentioned above.

e) Stark effect broadening in tubular pinch

As is clearly seen in Fig.8, the H_β, H_γ, and H_δ line spectra exhibit a large amount of line-broadening. It is another important problem for diagnostics of high temperature plasmas to trace the line contour. The electron density in a hot plasma is obtained from the Stark broadening of spectral emission lines. Therefore, many authors have already measured the line broadening in the case of hydrogen and helium discharges[8)]. The present streak camera with some modifications is also applicable to short-lived plasmas for time resolved studies of the line broadening.

A monochromatic image at the exit slit of the spectrograph is converted from a vertical line to a horizontal one on the film in the present device as mentioned in section (2). However, the horizontal line of image on the film can be oriented in the direction of sweep by the use of four mirrors instead of the three. A pair of the four mirrors controls a horizontal displacement of the image at the slit and the other pair does a vertical displacement, in order that the final image may be set at the central position on the film. If the light emission emerging from the discharge tube converges to a spot on the inlet slit, the final image on the film is also a spot, since such an optical arrangement is still anastigmatic. Then a line broadening can be recorded continuously during one discharge period.

In order to see the time variation of such line broadenings, one can set the two channels for H_β 4861Å and H_δ 4102Å, under the condition of the initial pressure at 1 torr of H_2 and the applied voltage at 15 kV. An example obtained is shown in Fig.10. The line broadening of H_β is roughly several tens Å. Fig.11 shows a microphotometric trace at 24 μsec after the emission started. The instrumental width is estimated at about 5Å for the present device.

f) AlI and ArII in wire explosion

An aluminum wire of one mm in diameter and 95 mm in length is stretched along the central axis of a large glass cylinder of 29 cm in diameter and 19 cm in length. Both ends of the stretched wire are screwed on copper stems fixed at copper plates. One of the copper plates is connected to a condenser bank of 100 μF through a vacuum switch, and the other has a square hole of 80 mm long and 10 mm wide to which a glass window is attached for observation.

The direction of view is along the wire axis and the middle part of the wire is focussed on the center of the inlet slit. The cylinder is evacuated in advance by an oil rotary pump and an argon gas is introduced at the pressure of 10 torr. When the condenser is charged up to 10 kV and the switch is triggered, an explosion of the aluminum wire takes place. The time-integrated emission spectrum consists of many lines due to AlI, ArII, and impurities such as CuI and CrI. Then the two channels of the streak camera are set for the strong emission lines of AlI 3961Å and ArII 4880Å.

The patterns obtained are shown in Fig.12. The streak patterns of the two different species are quite different from each other as seen in the figure, but these patterns seem to be composed of two stages. An early stage lasts about 6.6 μsec after an emission started and is followed by the stage of violent explosion. In the early stage, a weak emission is observed only at the position which corresponds to the wire axis on both channels. In the ArII pattern such an emission is too weak to be developed in a positive, but the negative plate really shows a weak emission. Bennett et al.[9)] and Chace[10)] have suggested that ohmic heating of a wire gives rise to phase transitions from solid through liquid to gas prior to explosion. The weak emission observed on both channels may be due to a continuous spectrum caused by heating up of the wire. In addition, the AlI pattern shows an overlapping of a slowly spreading motion, which may be due to spreading of Al vapor at this stage as pointed out by Conn[11].

When a violent explosion occurs, very fast expansions appear with strong emission. Although the expansion speed of AlI emission is nearly the same as that of ArII, other characteristics become different. In the case of Al, the fast expansion catches up with and passes through the slowly spreading Al vapor at about 7.6 μsec after the start of emission, and goes finally away from the range of observation, since the slit height does not cover the whole diameter of the glass cylinder at the present arrangement. On the other hand, the ArII pattern shows that a compression process starts on the way of the fast expansion at about 7.9 μsec after the start of the early stage. The compression is then followed by the second expansion.

According to Conn[11], a cylindrical shock wave produced by a violent expansion collides with the front of a slow expansion wave of a metallic vapor. As a result, the shock wave is partly reflected and partly propagates through the metallic vapor. The AlI pattern indicates the passing over of the fast expansion through the slowly spreading front of Al vapor. This fact possibly corresponds to the propagation of shock wave just cited above. However, an evidence about the reflection is difficult to be found on the AlI pattern. It should also be noted here that the compression process of ArII species starts nearly at the same time when the fast expansion collides with the slowly spreading front as seen in the AlI pattern. This fact may suggest that the compression process on the ArII pattern is related to the reflected shock wave.

Another difference between the behaviour of the two species lies in the period of emission. The AlI emission has a much longer life than the ArII emission, and shows an irregular repetition of expansion and compression processes with a long period of several tens μsec.

(4) Conclusion

A spectroscopic two-channel-streak-camera, which has been newly designed and constructed for the purpose of studying the breakdown in condensed discharges of various types, enables one to trace quick motions of different kinds of emitting species, simultaneously. In addition, this camera with some modification is applicable to condensed discharge plasmas for time resolved studies of the line broadening.

After its applications to the hot plasmas of a linear pinch, a tubular pinch, and a wire explosion caused by condensed discharges, it has been proved that the camera constructed is of good use for high temperature plasma diagnostics. Especially, it enables one to see how different kinds of species existent in a hot plasma behave in different manners of their own.

References

1) V.S.Komel'kov : Soviet Physics-JETP 35 (8)(1959) 10.

2) O.A.Anderson and W.B.Kunkel : Phys. of Fluids 12 (1969) 2099.

3) S.L.Leonard : Plasma Diagnostic Techniques edited by R.H. Huddlestone and S.L.Leonard (Academic Press, New York, 1965)

4) K.Ishii, H.Suemitsu and K.Fukuda : Japan. J. appl. Phys. 5 (1966) 1235.

5) A.H.Gabriel : Proc. Fourth Intern. Conf. Ionization Phenomena in Gases, Uppsala, 1959 Vol.2, p.829.
H.A.Bodin, N.J.Peacock and J.A.Reynolds : ibid Vol.2, p.861.

6) O.A.Anderson, W.R.Baker, J.Ise,Jr., W.B.Kunkel, R.V.Pyle and J.M.Stone : UCRL-8153, Jan. 1958.

7) T.Iwai, M.Ishigami, J.Yoda, H.Kumazawa and T.Horie : Japan. J. appl. Phys. 9 (1970) 516.

8) R.A.Hill and E.H.Beckner : Appl. Optics 3 (1964) 929.

9) F.D.Bennett, H.S.Burden and D.D.Shear : Phys. of Fluids 5 (1962) 102.

10) W.G.Chace : Phys. of Fluids 2 (1959) 230.

11) W.M.Conn : Phys. Rev. 98 (1955) A 1551.

Figure Captions

Fig.1 Spectroscopic two-channel-streak-camera.

Fig.2 Schematic diagram of the spectroscopic two-channel-streak-camera.

Fig.3 Time-integrated spectrum of linear pinch discharge in argon 1 torr, 10 kV.

Fig.4 Simultaneous tracings of motions of Na atom and Ar ion in linear pinch discharge in argon 1 torr, 10 kV.
CH 1 : NaI 5893Å, CH 2 : ArII 4880Å.

Fig.5 Simultaneous tracings of motions of Si ion and Ar ion in linear pinch discharge in argon 1 torr, 10 kV.
CH 1 : SiII 4128Å, CH 2 : ArII 4880Å.

Fig.6 Relative radial distribution of light intensity versus radius in the case of SiII at pinch time.

Fig.7 Simultaneous tracings of motions of Ar atom and Ar ion in tubular pinch discharge at various pressures of argon.
(a) 1 torr, (b) 3 torr, (c) 5 torr.
CH 1 : ArI 4300Å, CH2 : ArII 4880Å.

Fig.8 Time-integrated spectra in tubular pinch discharge.
(a) H_2O 0.5 torr, 15 kV, (b) H_2O 0.5 torr + Ar 2.5 torr, 15kV.

Fig.9 Simultaneous tracings of motions of H atom and Ar ion in tubular pinch discharge in H_2 0.5 torr + Ar 0.5 torr, 15 kV.
CH 1 : H_β 4861Å, CH 2 : ArII 4379Å.

Fig.10 Simultaneous tracings of line broadening in tubular pinch discharge in H_2 1 torr, 15 kV.
CH 1 : H_β 4861Å, CH 2 : H_δ 4102Å.

Fig.11 Microphotometric trace of H_β line contour at 24 μsec.

Fig.12 Simultaneous tracings of motions of Al atom and Ar ion in aluminum wire explosion at 10 kV into argon at 10 torr.
CH 1 : AlI 3961Å, CH 2 : ArII 4880Å.

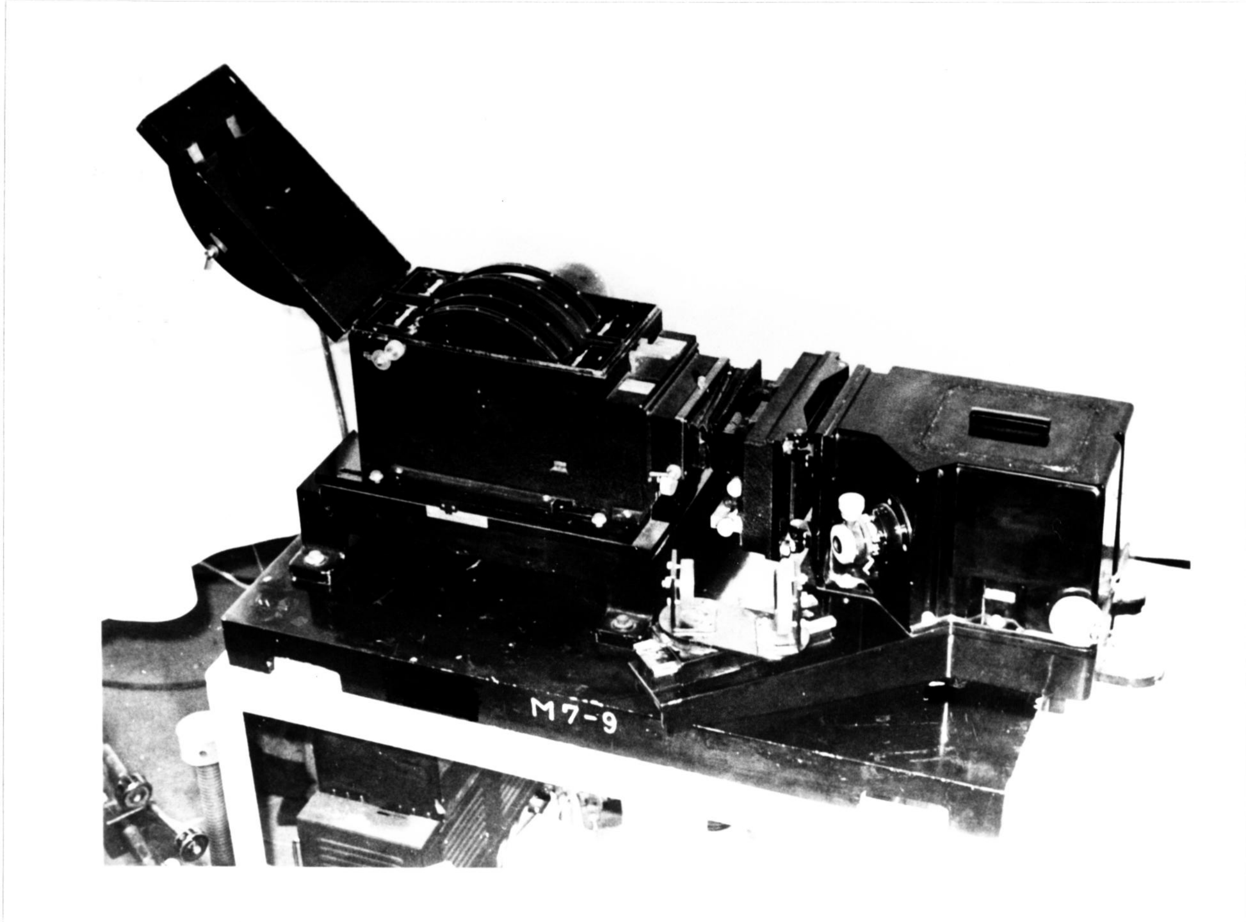

Fig.1

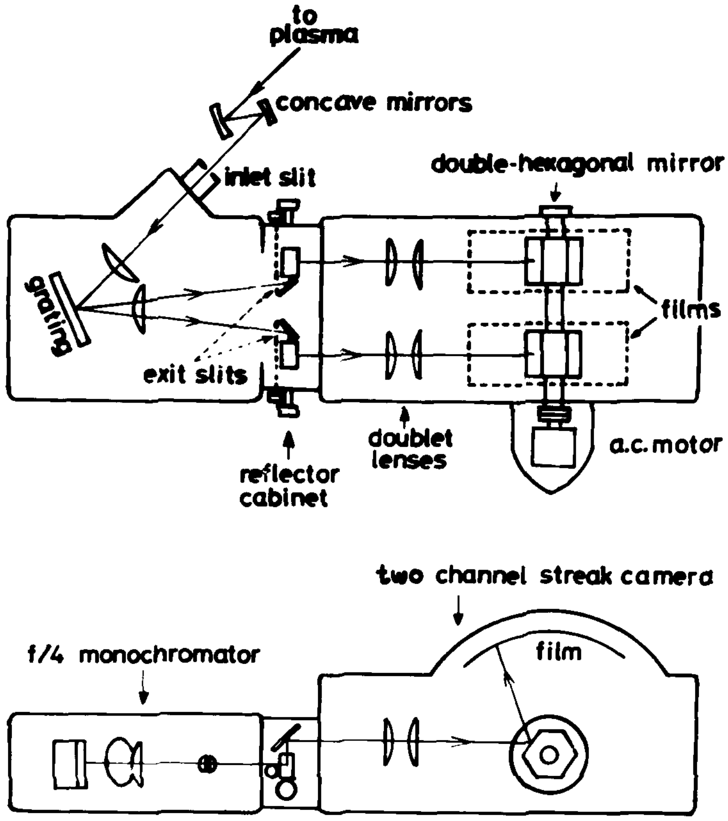
to plasma
concave mirrors
inlet slit
double-hexagonal mirror
grating
films
exit slits
reflector cabinet
doublet lenses
a.c. motor
two channel streak camera
f/4 monochromator
film

Fig.2

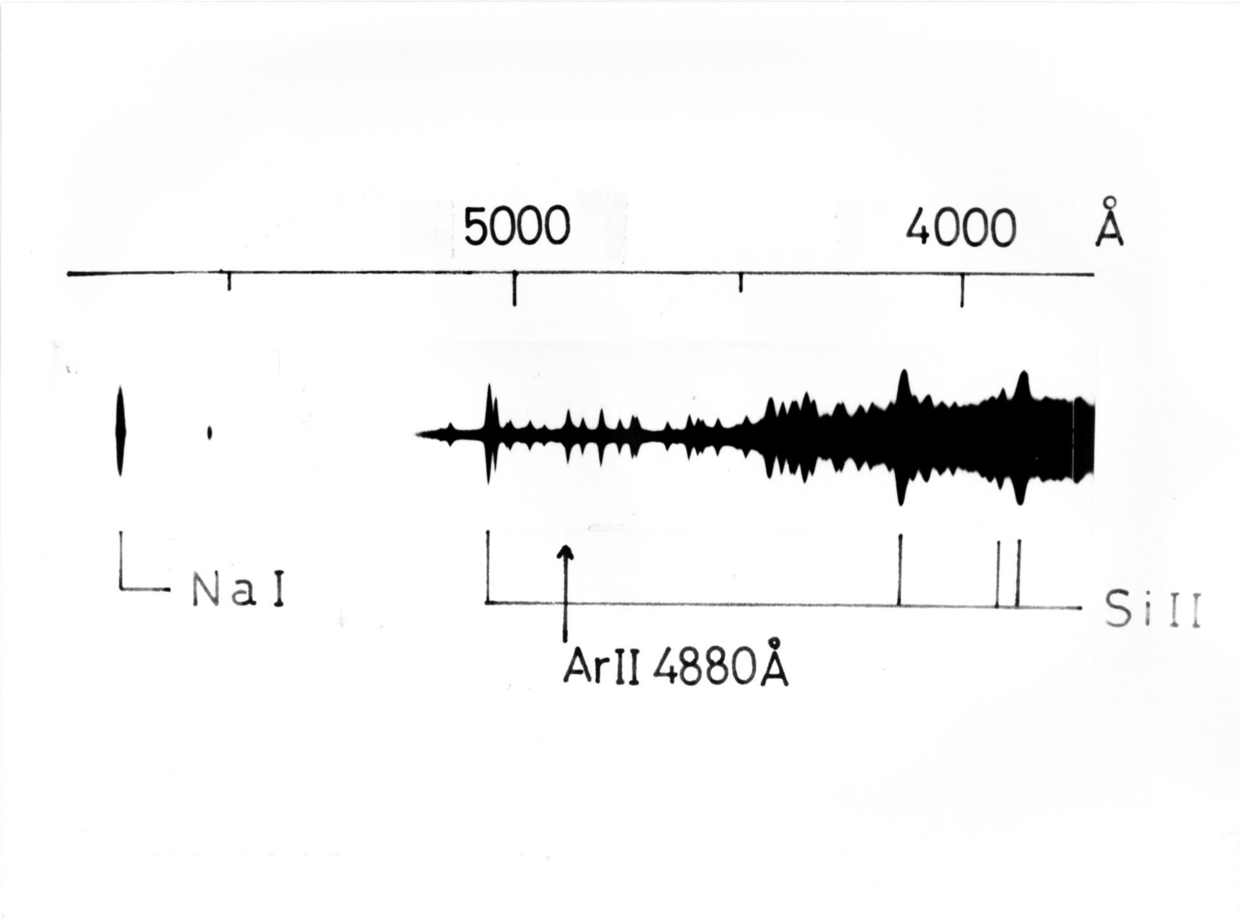

Fig.3

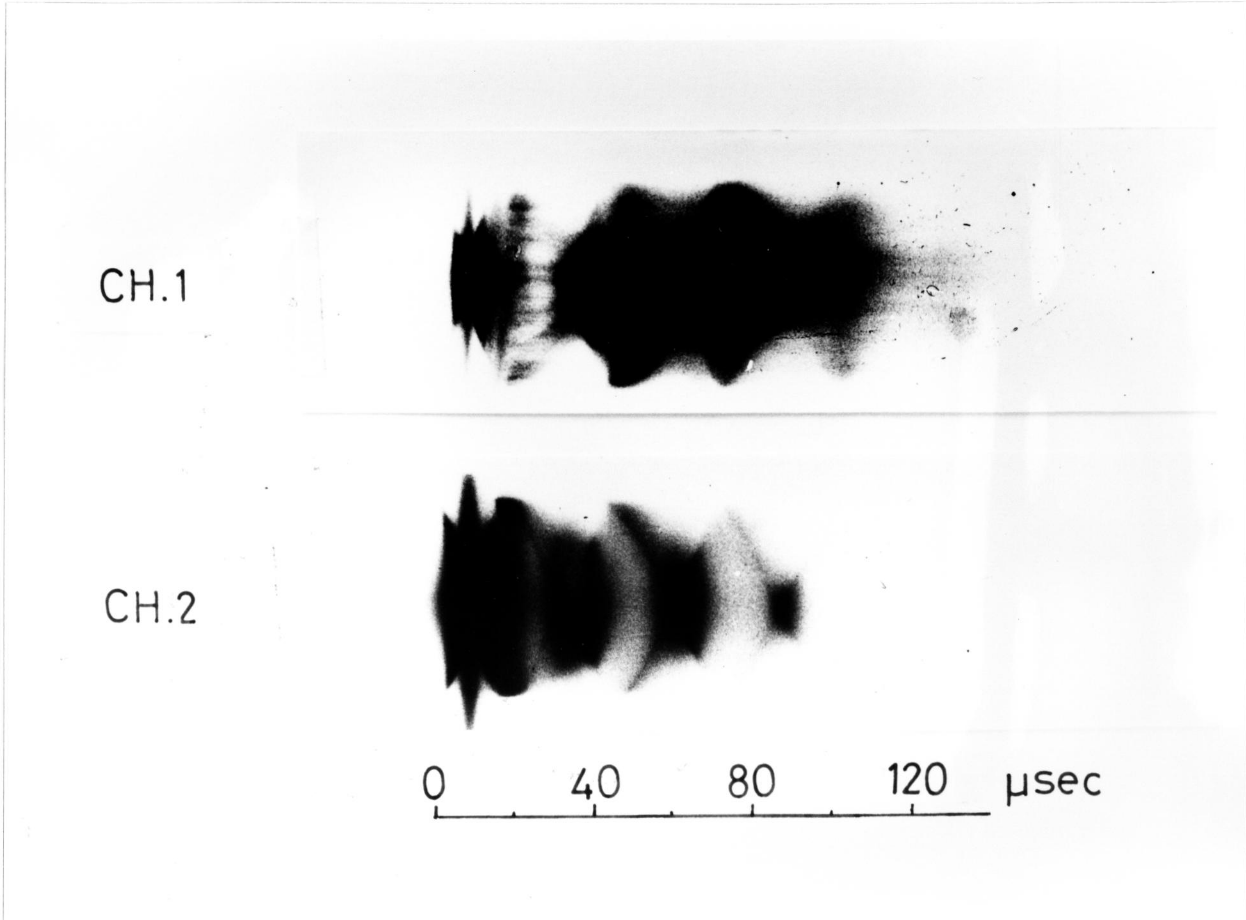

Fig.4

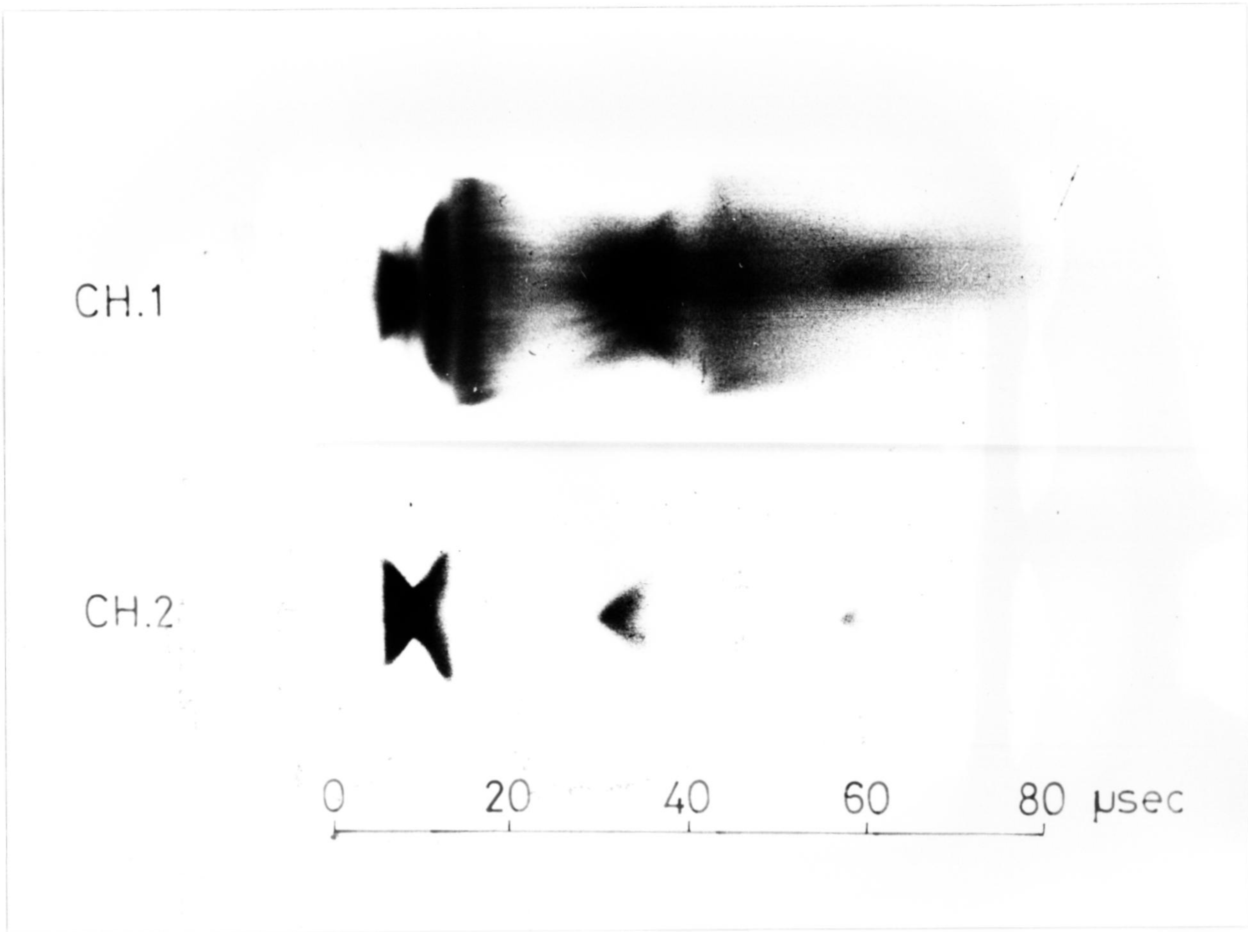

Fig.5

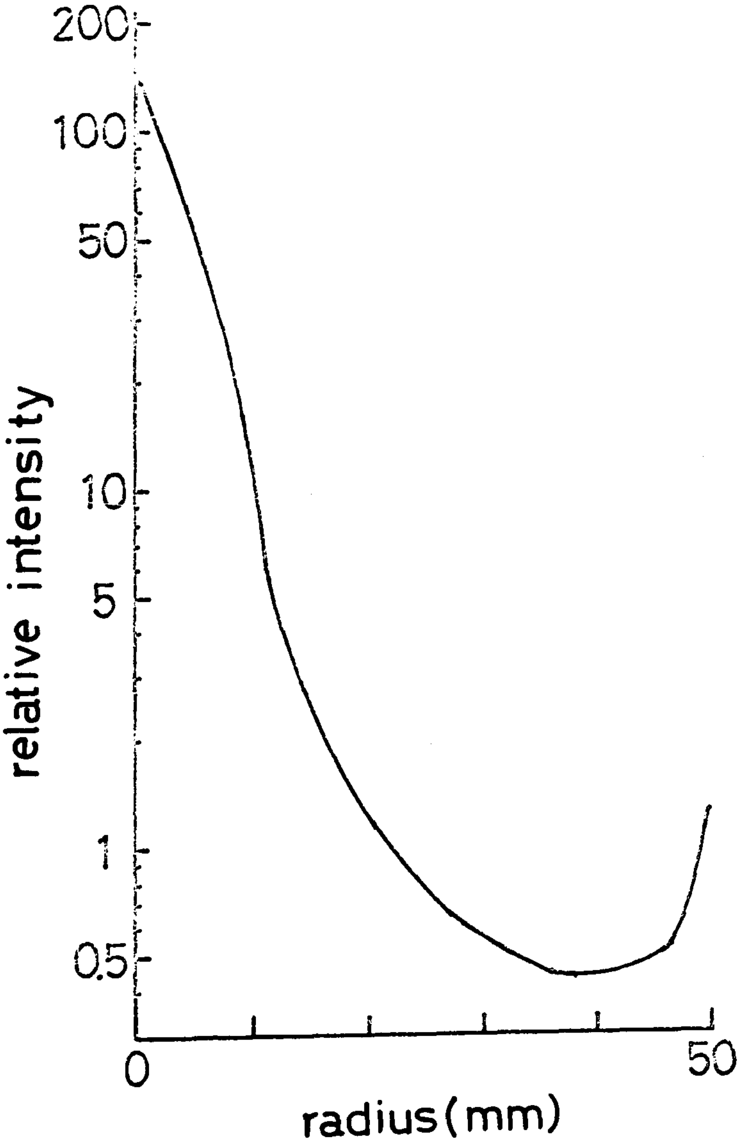

Fig.6

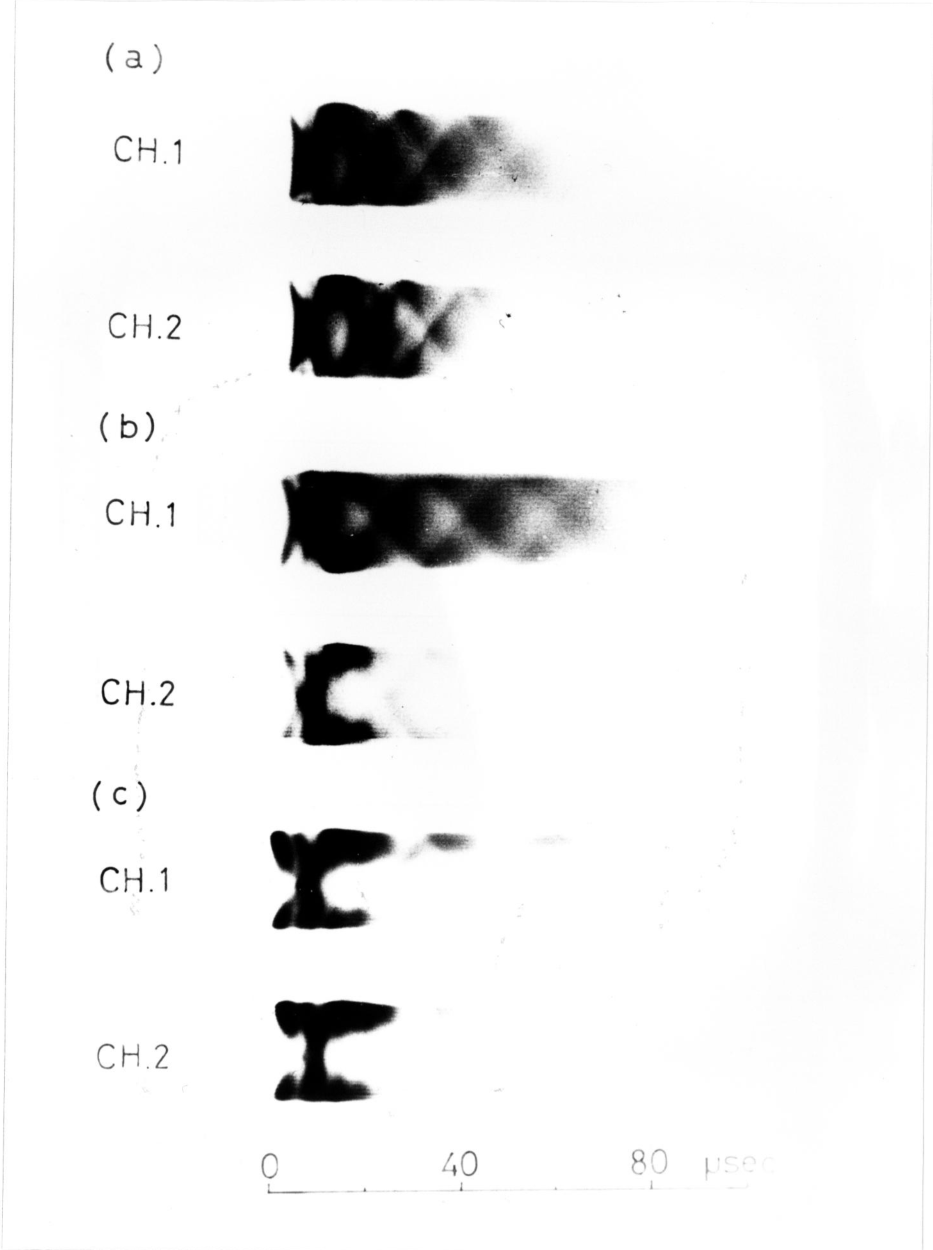

Fig.7

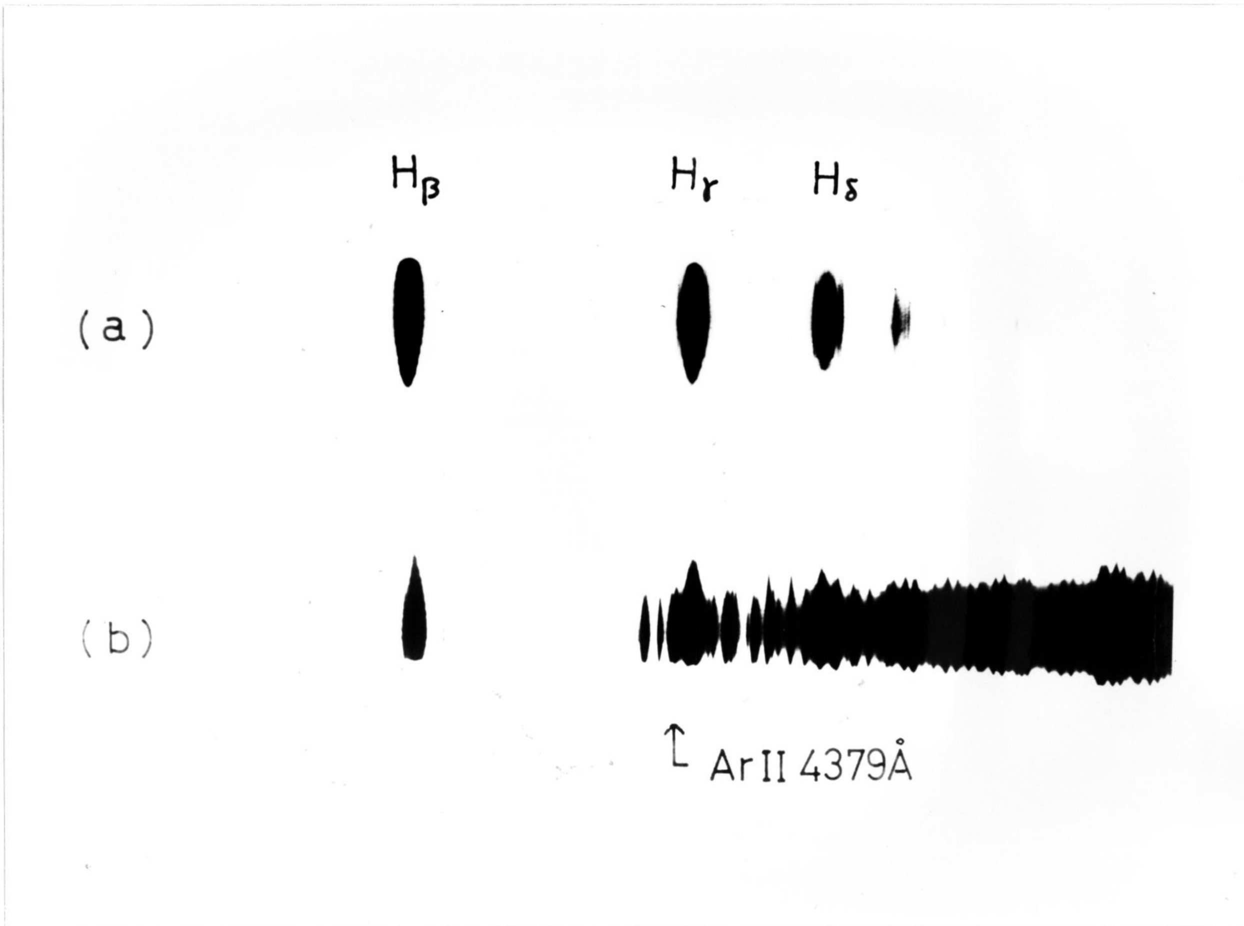

Fig.8

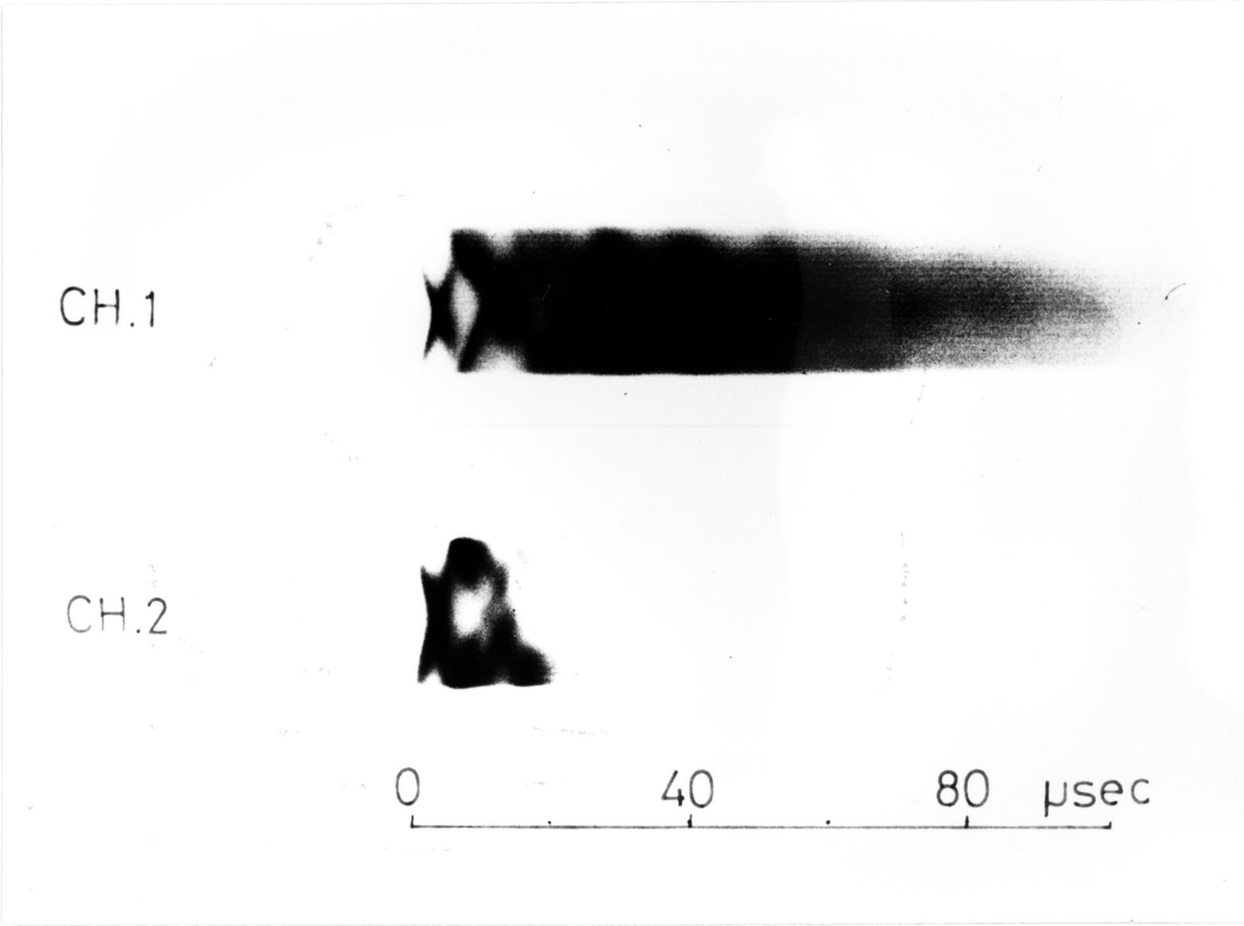

Fig.9

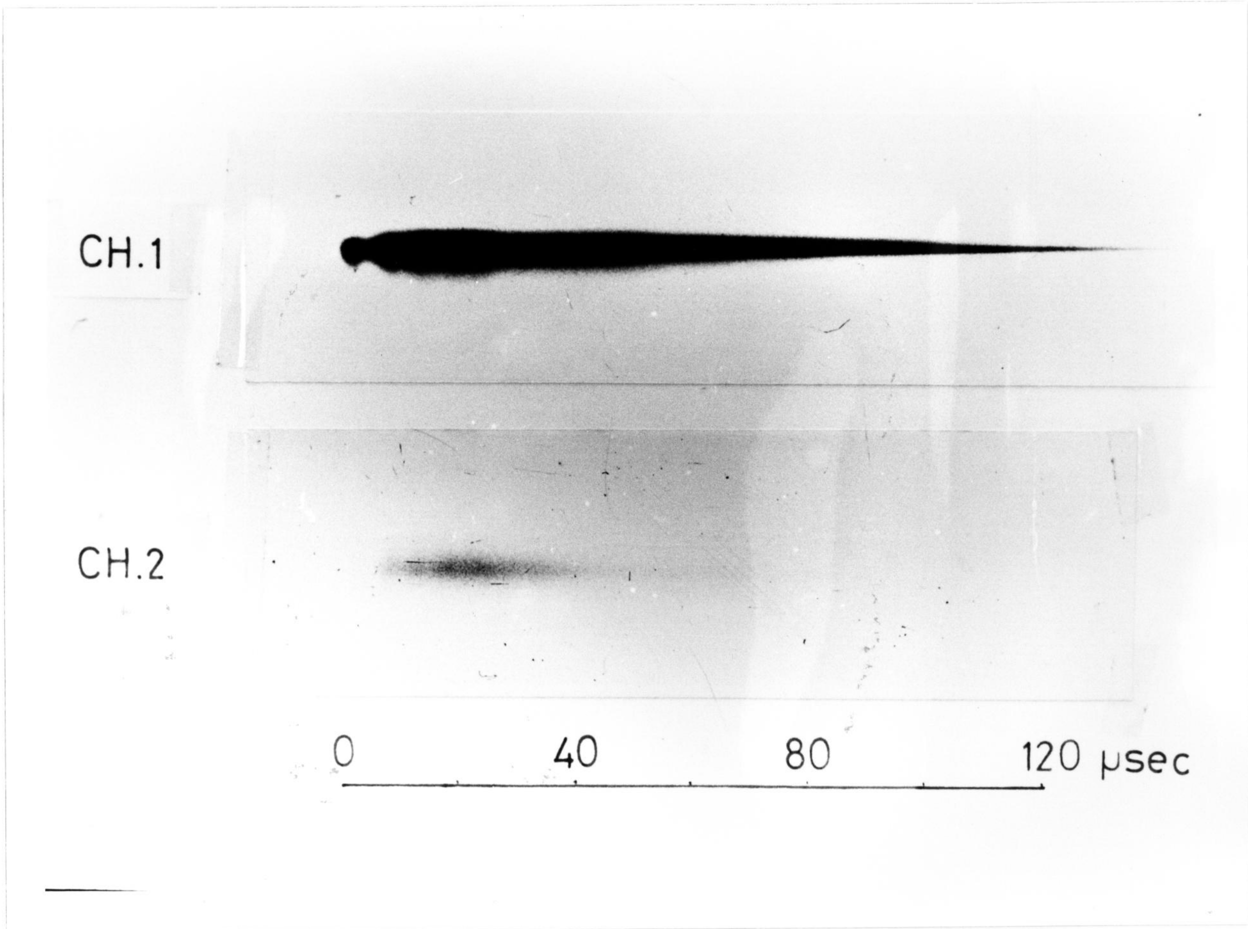

Fig.10

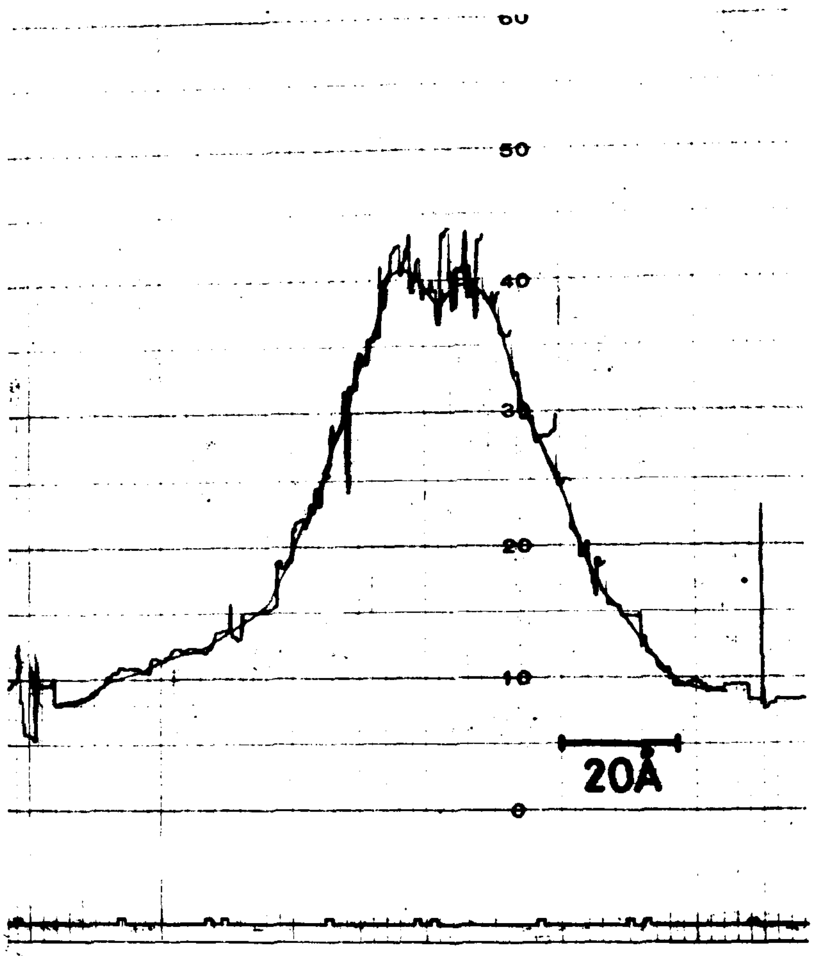

Fig.11

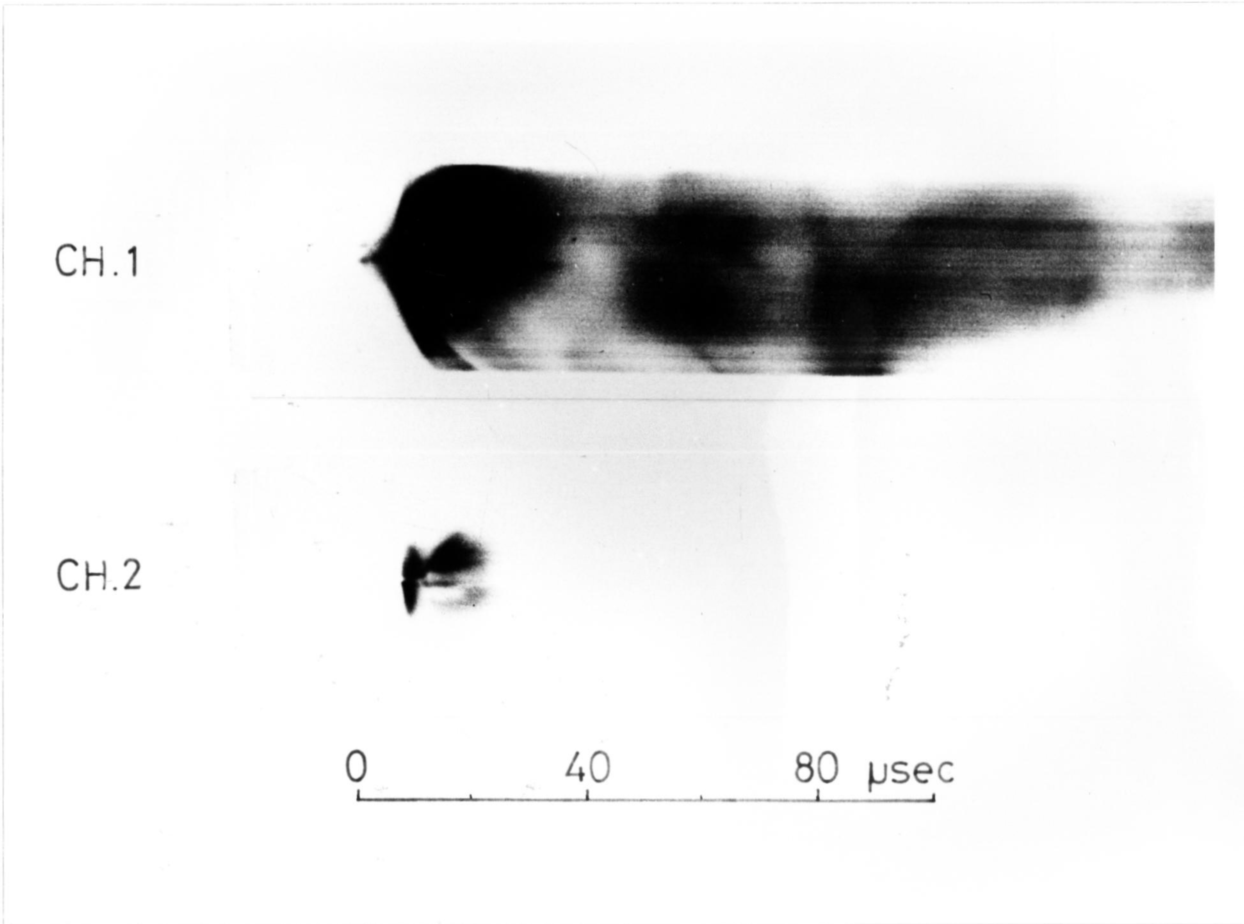

Fig.12

PART II

TIME RESOLVED STUDIES ON LASER ACTIONS

1. Time Resolved Behaviour of Singly and Doubly Ionized Argon Ion Laser Lines

(1) Introduction

The excitation mechanism for the argon ion laser is a problem that has been studied by many authors for years. For explanation of the cw or quasi-cw lasering of Ar^+, two-step excitation processes via the ionic ground state[1], the ionic metastable state[2], or the neutral metastable state[3] have so far been proposed. In addition, cascade transitions from highly excited levels to the upper laser levels have been suggested to play an important role in the laser action[4]. On the other hand, concerning the pulsed operation, a direct excitation process from the neutral ground state to an upper laser state of singly ionized argon has been proposed by Bennett[5]. It is the so-called "sudden perturbation theory"[6].

In the present experiment carried out with an extremely high current pulsed discharge tube ($\sim$2kA), two different laser pulse modes have been confirmed. The primary laser pulse composed of the line 4765 of ArII, the lines 3511 and 3638 of ArIII occurs at the early stage of the discharge. On the other hand, the secondary laser pulse, which consists only of the line 4880 of ArII, takes place in the afterglow of the discharge. In what follows, the time resolved behaviour of these laser lines will be studied in detail under various discharge conditions. After that, an excitation mechanism will be newly proposed for explanation of all the experimental results obtained.

(2) Experimental procedures

A Pyrex discharge tube used is 140 cm in length, 5 mm in diameter, and both of its ends are sealed with fused quartz Brewster angle windows. The laser cavity consists of an aluminum-coated plane mirror and an aluminum-coated spherical mirror whose radius of curvature is 400 cm. The mirrors are separated by a distance of 160 cm. Laser action is obtained with pulsed discharges between cold nickel electrodes located in side arms at both ends of the tube, into which 99.99 percent pure argon gas is admitted after evacuation by an oil diffusion pump down to about 10^{-5} torr.

The laser beam, through the plane mirror, is led into an entrance slit of a monochromator. Variation in intensity of each one of the four laser lines is obtained with a photomultiplier of RCA 1P28, which is connected directly to a dual beam cathode ray oscilloscope.

The total laser output is also quite variant. The laser beam is partly reflected sideward by a half-silvered mirror set on the path of the beam. Change in intensity of the reflected beam is traced by a phototube and the oscilloscope. In addition, change in intensity of the spontaneous emission radiated outside the tube is traced by use of another phototube and the oscilloscope.

Condensed discharges through argon are powered by a 2 μF capacitor bank charged up to 15 kV. Variation of the discharge current is observed by its voltage drop across a low inductance resistor. Quick change of the voltage between the electrodes is measured by use of a divider. The block diagram of the experimental set-up is shown in Fig.1.

(3) Experimental results

The time-integrated laser spectra are presented in Fig.2, as a function of the starting pressure and the applied voltage. At the pressure of 18 mtorr and the applied voltage of 8 kV, all the four laser lines exhibit themselves at 3511, 3638, 4765, and 4880 Å, as shown in Fig.2(a). When the applied voltage is raised under the same pressure as above, only the laser line 4880 fails to occur, as shown in Fig.2(c). On the contrary, when the voltage is kept constant at 12 kV and the pressure is raised from 15 to 23 mtorr, the laser action of the line 4880 is gradually enhanced, as shown in Fig.2(b) to (e). Visual intensities of the four lines are intuitively plotted against pressures in Fig.3.

The transitions for the laser lines observed and the term symbols for the levels concerned are shown in Fig.4 on the basis of the tabulated energy levels presented by Moore.[7] Although the identification of the transition for the line 3638 of ArIII has been suggested by McFarlane as shown in the same figure, the energy levels for them are not yet known numerically, and accordingly they are indicated by the dotted lines.[8]

In Fig.5, the time resolved behaviour of the four laser lines are shown. The upper trace in each one of the figures shows the laser pulse and the lower trace the spontaneous emission through the side wall of the laser tube. The sweep rate is 5 μsec per division. The waveforms of the discharge current I, the discharge voltage V, and the total laser output P_L are compared with each other in Fig.6.

The time interval, ΔT, between the first laser pulse and the second becomes longer as increasing the discharge voltage and decreasing the pressure, as shown in Fig.7. Both the voltage effect and the pressure effect may be closely related to the electron temperature in the argon plasma.

After a few tens shots of pulse discharges through the filled gas, instead of admitting fresh gas for each shot, the colour of the laser beam turns gradually green to blue. From the viewpoint of the spectra, the line 4880 is most dominant in the laser beam at the initial stage, while the line 4765 becomes more dominant than the rest at the final stage. Such a change may be due to impurities outgased by condensed discharges repeated many times.

Superposition of a high frequency field upon the condensed discharge brings about a significant effect especially to the line 4880. The high frequency field ($\sim$10 MHz) is applied to the laser tube with external electrodes as shown in Fig.1. When excited only by the condensed discharge, the lines 4765 and 4880 exhibit strong enhancements in the respective moments, as shown in Fig.8(a) and Fig.8(b). When the high frequency field is superimposed upon the condensed discharge, sudden changes take place in intensities of both the lines 4765 and 4880, as shown in Fig.8(c) and Fig.8(d), respectively. The maximum intensity of the line 4765 increases more or less, while the line 4880 does fail to appear throughout the discharge.

(4) Newly proposed excitation process for the line 4880

The first laser pulse takes place at the early stage of the condensed discharge, and it is composed of the lines 4765 of ArII, and 3511, 3638 of ArIII. It shows a rapid rise in intensity and disappears while the condensed discharge lasts. On the other hand, the second laser pulse composed only of the line 4880 of ArII appears only in the afterglow of the condensed discharge. The latter shows a little slow rise. At a glance of these characteristics, there seems to be two different excitation processes, each of which contributes to the primary and the secondary pulse mode, respectively.

The laser action of the line 4765 is not so sensitive to the impurity effect as the line 4880 is. Moreover, the line 4765 is enhanced a little even when the high frequency field is superposed upon the condensed discharge. In addition, the laser action of the line 4765 is prominent under the condition of higher voltages and lower pressures. Such evidences stand by the direct excitation process for the line 4765, that is the so-called "sudden perturbation theory" proposed by Bennett, as shown in Fig.9(a). According to this process, the main yield of the excited Ar^+ ion will occur in the 4p $^2P^\circ_{3/2}$ state, and the most part of the gain will be expected on the line 4765, which is in good agreement with the present results.

In the spontaneous emission spectrum, the doubly ionized argon lines 3511 and 3638 are both much more intense than the line 4765 [see Fig.2(f)] . In addition to this, there are several other experimental evidences which lead to an expectation that a good deal of doubly ionized argon ions exist in the plasma, at least, at the early stage of the condensed discharge. In Fig.5, it is shown that the time resolved behaviours of the lines 3511 and 3638 are nearly the same as that of the line 4765. More strictly, however, the appearance time of the peak intensity of the former seems to be a little late compared with that of the latter.[9)] As for the excitation processes for these lines, nearly the same direct excitation process as above may be applied[10)], where the singly ionized argon is supposed to be re-ionized and excited simultaneously by fast moving electron impact. As it will take time to produce a sufficient number density of Ar^{++}, such a delay time may exist.

On the other hand, the strikingly delayed appearance of the line 4880 together with the high frequency field effect and the impurity effect may strongly suggest that a certain metastable state is related to the excitation process for the line 4880. Actually, there are several ionic metastable states, $^2F_{7/2}$, $^4F_{7/2}$, $^4F_{9/2}$ and

$^4D_{7/2}$, the energy levels of them being at 34.25, 33.45, 33.38, and 32.16 eV above the ground state of the argon atom.[11] These metastable states are denoted en bloc by Ar^{+m} in Fig.9.

The upper level for the line 4880, $^2D^\circ_{5/2}$, is at 35.44 eV above the ground state of the argon atom, and it is just above Ar^{+m} only by a few eV, as seen in Figs.4 and 9. The electron temperature in the afterglow can be estimated at ~ 1 eV with conductivity. According to Spitzer,[12] the conductivity in plasma, σ, is expressed as follows, $\sigma^{-1} = 6.53 \times 10^3 (\ln\Lambda / T_e^{3/2})$, where T_e is the electron temperature, Λ the ratio of the Debye shielding distance to the value of impact parameter, and $\ln\Lambda = 10$ for the argon plasma under discussion.[13] Therefore, it is most probable for the metastable ions to be pumped up to the laser level, $^2D^\circ_{5/2}$, by collisions of electrons with low energies of a few eV.

By the way, the upper level for the line 4765, $^2P^\circ_{3/2}$, is at 35.63 eV above the ground state of the argon atom. The energy difference between the levels $^2P^\circ_{3/2}$ and $^2D^\circ_{5/2}$ is so small as 0.19 eV that it is impossible to explain the reason why the level $^2D^\circ_{5/2}$ is preferable to the level $^2P^\circ_{3/2}$ for the collisional pumping, only by taking energies into consideration. However, this question can be settled down, if the selection rules are applied. The general selection rules, $\Delta S=0$, $\Delta L=0, \pm 1$, $\Delta J=0, \pm 1$, permit only the transition from Ar^{+m} to the level $^2D^\circ_{5/2}$.[14)]

Generally, the cross-section for excitation of an optically allowed transition shows a maximum at an energy as high as 3 to 4 times the threshold. On the contrary, the excitation function for an optically forbidden transition does a maximum very close to the threshold and decreases rapidly at high energies. Moreover, the magnitude of the cross-section for the former transition is several tens times greater than that for the latter.[15)] In addition, the cross-section for the electron-ion recombination is negligibly small, because of the electron temperature, which is relatively high in the afterglow of the discharge.[16)] As a result, the transition from Ar^{+m} (especially from the level $^2F_{7/2}$) to the level $^2D^\circ_{5/2}$ is most important among other transitions.

(5) Conclusion

As far as the line 4880 is concerned, it is convenient to assume another process for its lasering in the afterglow of the discharge. At first, doubly ionized argon ions are produced abundantly at the early stage of the condensed discharge. Soon after that, they will in part come down to the metastable states denoted en bloc by Ar^{+m} through recombination and cascade transitions, as shown in Fig.9(b). The electron temperature in the afterglow, which can be estimated at about 1 eV, may be effective for pumping of argon ions from Ar^{+m} to the $^2D^\circ_{5/2}$ level.

Qualitatively, when the discharge voltage is raised, or the pressure lowered, the electron temperature may be expected to increase. As a result, the newly proposed process leading to the $^2D^\circ_{5/2}$ level will be suppressed till the electron temperature decreases, and incidentally, the time interval ΔT will change, as shown in Fig.7.

When the high frequency field is superimposed, the electron temperature is so high that the line 4880 becomes missing, as shown in Fig.8. As for the impurity effect, it has already been shown by Sokabe that the metastable state in the argon afterglow is quite sensitive to the collisional quenching by impurities.[17]

(6) Remarks

Some comments should be added here with respect to the dielectric-coated mirror effect. When the dielectric-coated mirrors were used in place of the aluminum-coated ones, six laser lines, 4579, 4765, 4880, 4965, 5017 and 5145 of ArII could be obtained. Each of the dielectric-coated mirrors used has reflectivity of 100 percent and 92 percent at 4880Å, respectively, and 3 percent decrease of reflectivity at 5400Å and 4300Å. In addition, the laser action of the line 4880 took place in two different moments, one at the early stage and the other in the afterglow of the discharge. The peak intensity of the primary pulse was weaker than that of the secondary one.[18~20]

On the other hand, the laser actions of the other five lines occured only at the early stage of the discharge. The time resolved behaviour of the lines 4880 and 4765 are shown in Fig.10. The upper trace in each one of the figures shows the total laser output. When the high frequency field was superimposed upon the condensed discharge, the primary pulse of the line 4880 was not missing, while the secondary pulse failed to appear, as shown in Fig.11.

Needless to say, such a behaviour of the line 4880 quite different from that described in the preceding sections must have been attributed to the decrease in the optical losses at the mirrors. The excitation mechanism for the primary pulse of the line 4880 has been discussed by Smith and Dunn from the stand-point of the direct excitation process.[21)] The secondary pulse of the line 4880 must be due to the indirect excitation process proposed in the present paper.

References

1) E.F.Labuda, E.I.Gordon and R.C.Miller : IEEE J. Quantum Electronics QE-1 (1965) 273.

2) E.I.Gordon, E.F.Labuda, R.C.Miller and C.E.Webb : Physics of Quantum Electronics, ed. P.Kelley, B.Lax and P.Tannenwald (McGraw-Hill, New York, 1966) p.664.

3) W.R.Bennett,Jr. : Chemical Lasers, Appl. Optics Suppl. 2 (1965) p.3.

4) R.I.Rudko and C.L.Tang : Appl. Phys. Letters 9 (1966) 41.

5) W.R.Bennett,Jr., J.W.Knutson,Jr., G.N.Mercer and J.L.Detch : Appl. Phys. Letters 4 (1964) 180.

6) W.E.Lamb,Jr. and M.Skinner : Phys. Rev. 78 (1950) 539.

7) C.E.Moore : Atomic Energy Levels, Vol.1 (National Bureau of Standards, Washington,D.C., 1949).

8) R.A.McFarlane : Appl. Optics 3 (1964) 1196.

9) Y.Hashino, Y.Katsuyama and K.Fukuda : Japan. J. appl. Phys. 11 (1972) 907.

10) P.K.Cheo and H.G.Cooper : J. appl. Phys. 36 (1965) 1862.

11) H.D.Hagstrum : Phys. Rev. 104 (1956) 309.

12) L.Spitzer,Jr. : Physics of Fully Ionized Gases (Wiley, New York, 1961), p.139.

13) C.B.Zarowin : Appl. Phys. Letters 15 (1969) 36.

14) G.Herzberg : Atomic Spectra and Atomic Structure (Dover, 2nd. Ed., 1944), Chapter 4.

15) H.S.W.Massey, E.H.S.Burhop and H.B.Gilbody : Electronic and Ionic Impact Phenomena, 2nd. Ed. (Oxford University Press, 1969), Vol.1 Chapter 4.

16) A.Funahashi and S.Takeda : J. Phys. Soc. Japan 27 (1969)182 ; A.Funahashi, T.Makihira and S.Takeda : J. Phys. Soc. Japan 29 (1970)441.

17) N.Sokabe : Ph. D. Thesis. Osaka University 1971.

18) W.Demtröder : Phys. Letters 22 (1966) 436.

19) S.Kobayashi, K.Ujihara and M.Kamiyama : IEEE J. Quantum Electronics QE-2 (1966) 699.

20) M.B.Klein : Appl. Phys. Letters 17 (1970) 29.

21) A.L.S.Smith and M.H.Dunn : IEEE J. Quantum Electronics QE-4 (1968) 838.

Figure Captions

Fig.1 A schematic view of the experimental arrangement. P.M.,photomultiplier; M.,monochromator; H.M.,half-silvered mirror; P.T.,phototube; C.R.O.,cathode ray oscilloscope; H.F.,high frequency field supply; H.V.,dc high voltage power supply; T,trigger; C,capacitor bank; R,low inductance resistor.

Fig.2 Argon ion laser spectra (a) ~ (e) and spontaneous emission spectrum (f).
a) 8kV, 18mtorr. b) 12kV, 15mtorr. c) 12kV, 18mtorr. d) 12kV, 20mtorr. e) 12kV, 23mtorr. f) typical spontaneous emission spectrum, 10kV, 23mtorr.

Fig.3 Plots of visual intensity versus pressure for the four laser lines observed at 12kV.

Fig.4 The energy level diagram for the observed argon ion laser transitions. The energy levels indicated by the dotted lines are not yet known numerically.

Fig.5 Time resolved behaviour of the laser lines (upper trace) and the spontaneous emission (lower trace) at 6kV, 18mtorr. Sweep:5μsec/div.

Fig.6 The waveforms of the discharge current I, the discharge voltage V, and the total laser output P_L.
Sweep : 5μsec/div.

Fig.7 Time interval ΔT versus applied voltage, under pressures of 22 and 31 mtorr.

Fig.8 High frequency field effects to the laser lines 4765 and 4880Å, where lower traces show the discharge current.
a), b);laser actions excited only by the condensed discharge.
c), d);laser actions excited by the high frequency field superimposed upon the condensed discharge.
Sweep:5μsec/div.

Fig.9 Excitation processes.
a) The direct excitation process for 4765Å proposed by Bennett.
b) The newly proposed excitation process for 4880Å.

Fig.10 Time resolved behaviour of the laser lines 4880 and 4765 in comparison with the total laser output P_L, when the dielectric-coated mirrors are used.
Sweep:10μsec/div.

Fig.11 High frequency field effects to the laser lines 4765 and 4880Å, when the dielectric-coated mirrors are used.
Lower traces show the discharge current. Sweep:5μsec/div.

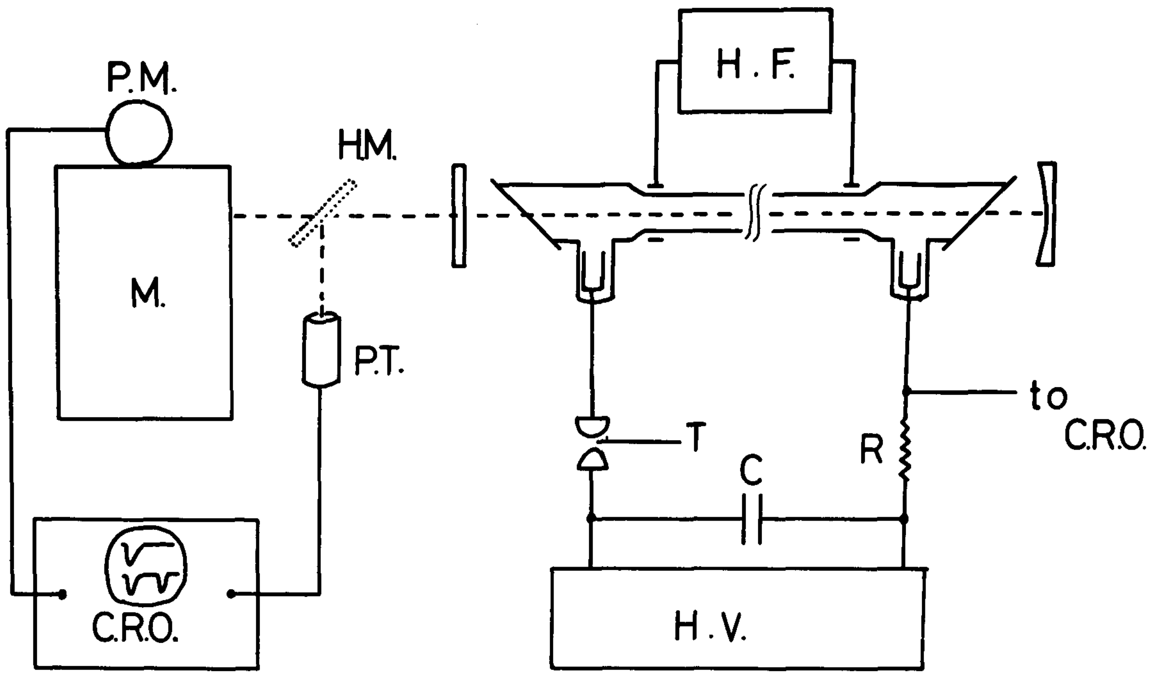

Fig.1

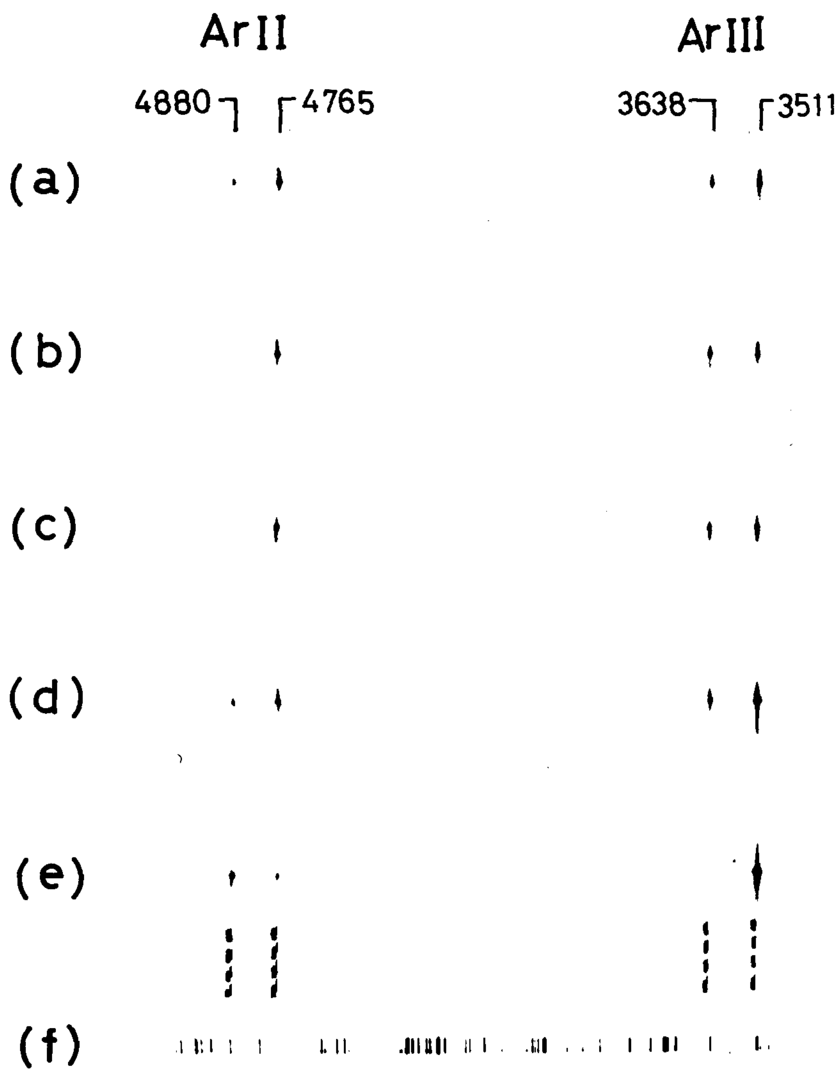

Fig.2

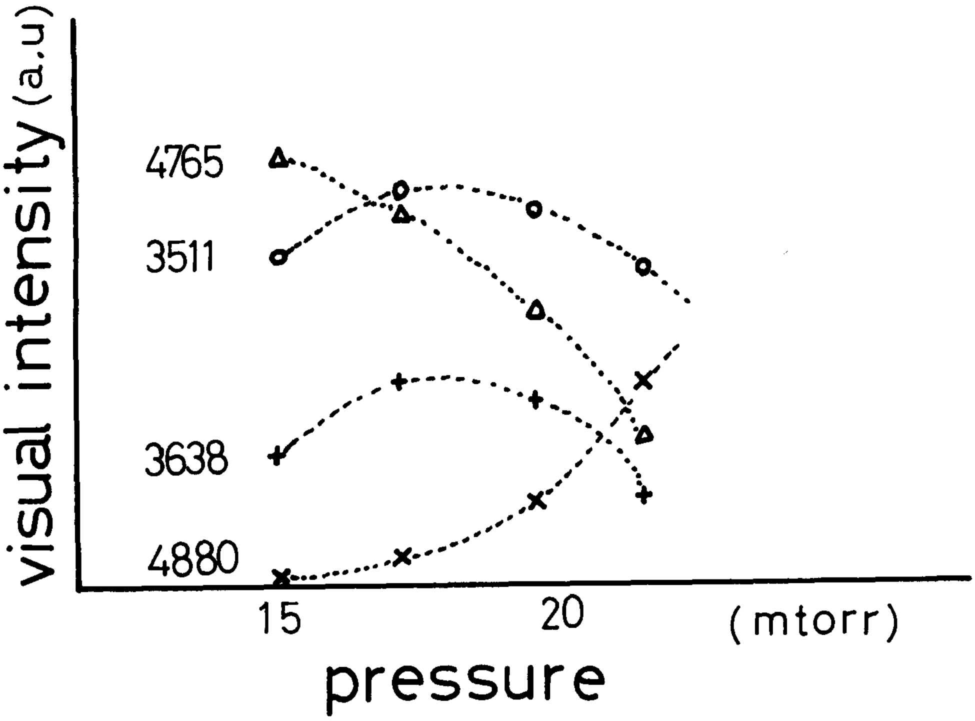
visual intensity (a.u)
4765
3511
3638
4880
15
20
(mtorr)
pressure

Fig.3

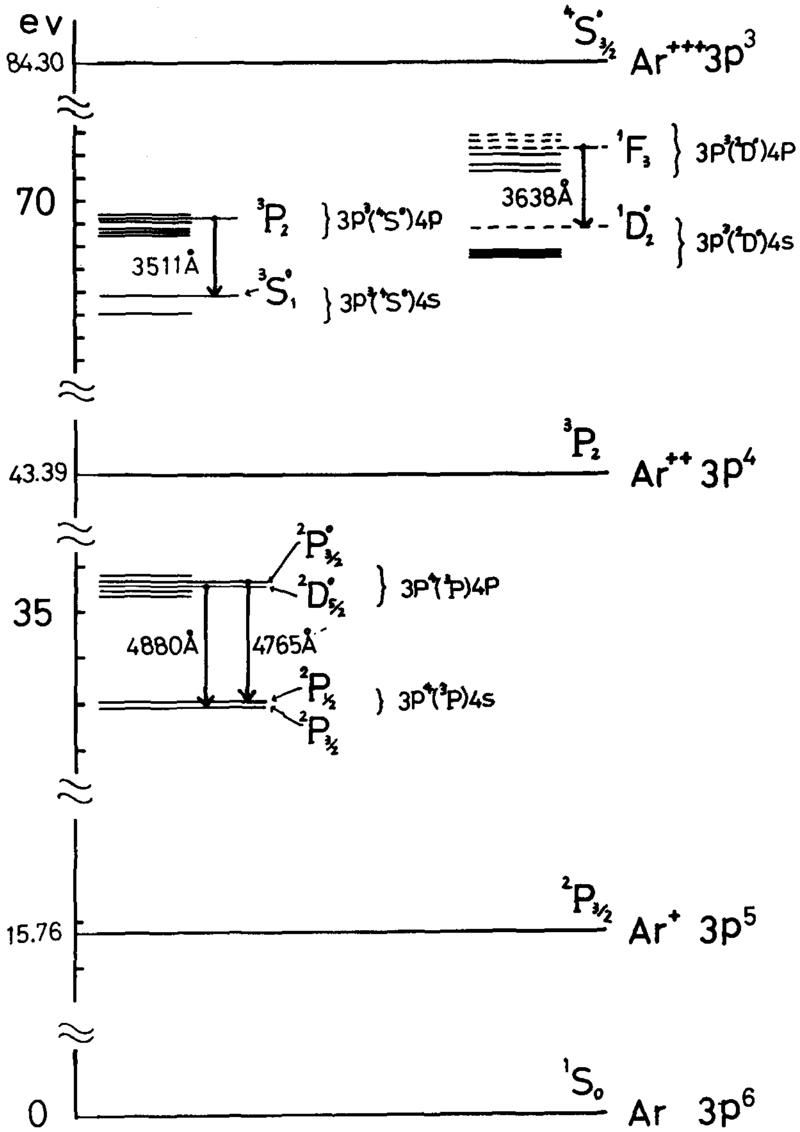

ev
84.30
70
35
43.39
15.76
0
${}^4S^\circ_{3/2}$ Ar^{+++}3p^3
${}^1F_3$ } 3P^3(^{2}D$^\circ$)4P
3638Å
${}^1D^\circ_2$ } 3P^3(^{2}D$^\circ$)4s
${}^3P_2$ } 3P^3(^{4}S$^\circ$)4P
3511Å
${}^3S^\circ_1$ } 3P^3(^{4}S$^\circ$)4s
${}^3P_2$ Ar^{++} 3P^4
${}^2P^\circ_{3/2}$
${}^2D^\circ_{5/2}$ } 3P^4(^{3}P)4P
4880Å
4765Å
${}^2P_{1/2}$ } 3P^4(^{3}P)4s
${}^2P_{3/2}$
${}^2P_{3/2}$ Ar$^+$ 3p^5
${}^1S_0$ Ar 3p^6

Fig.4

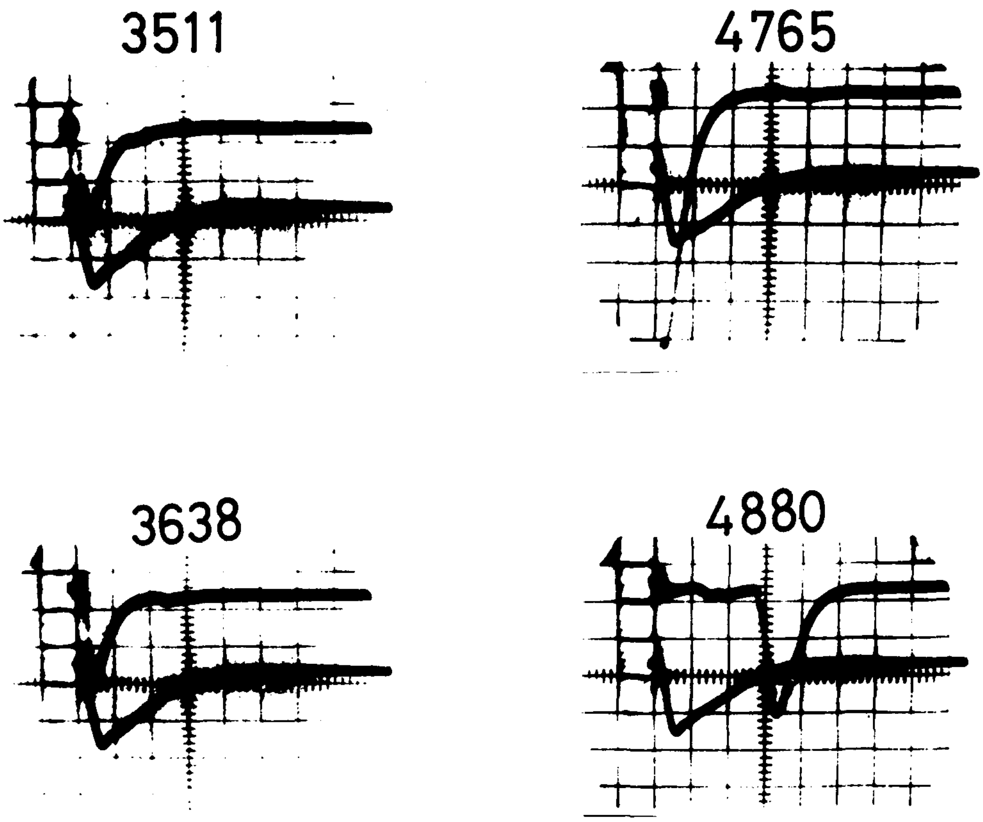

Fig.5

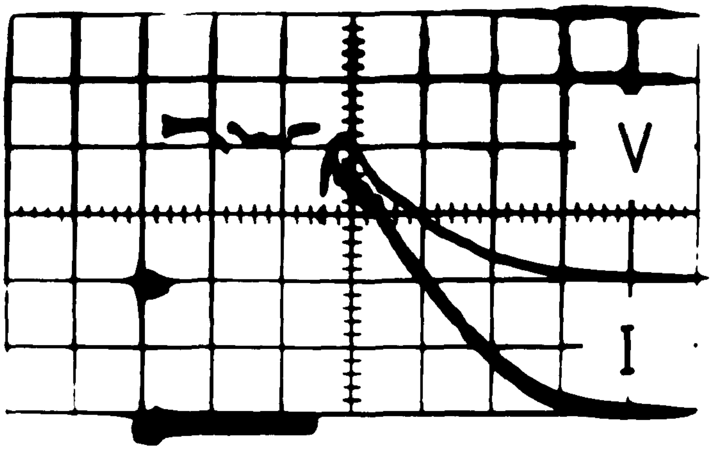

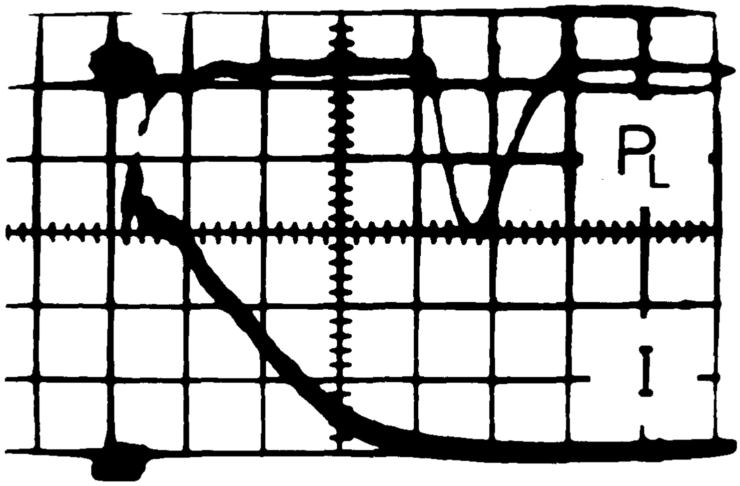

Fig.6

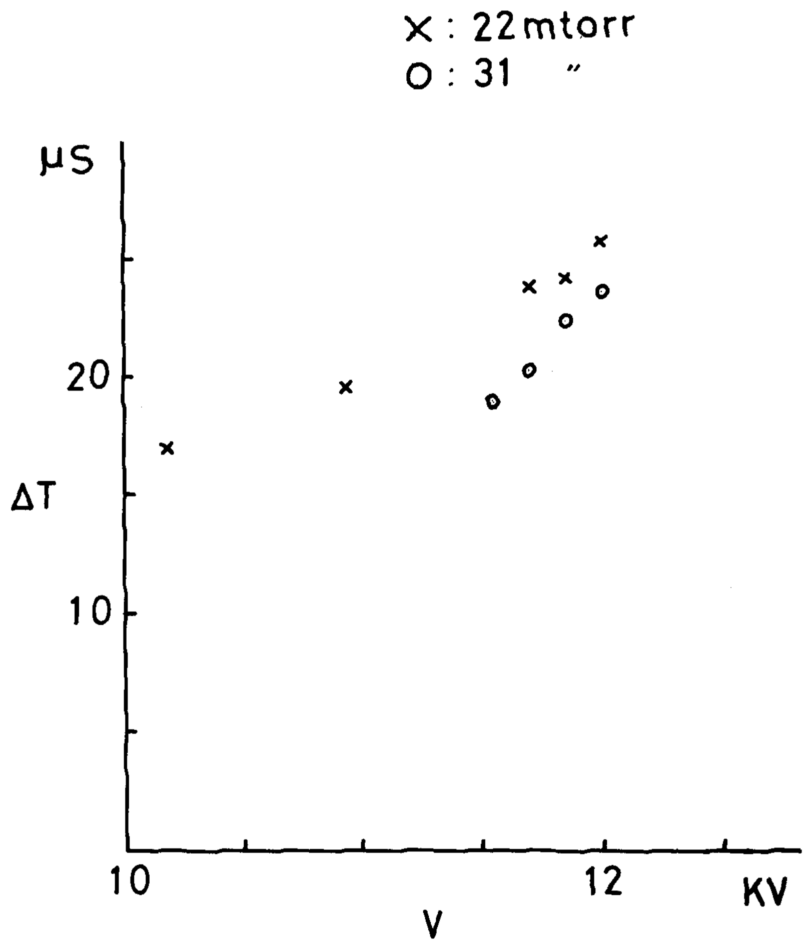

Fig.7

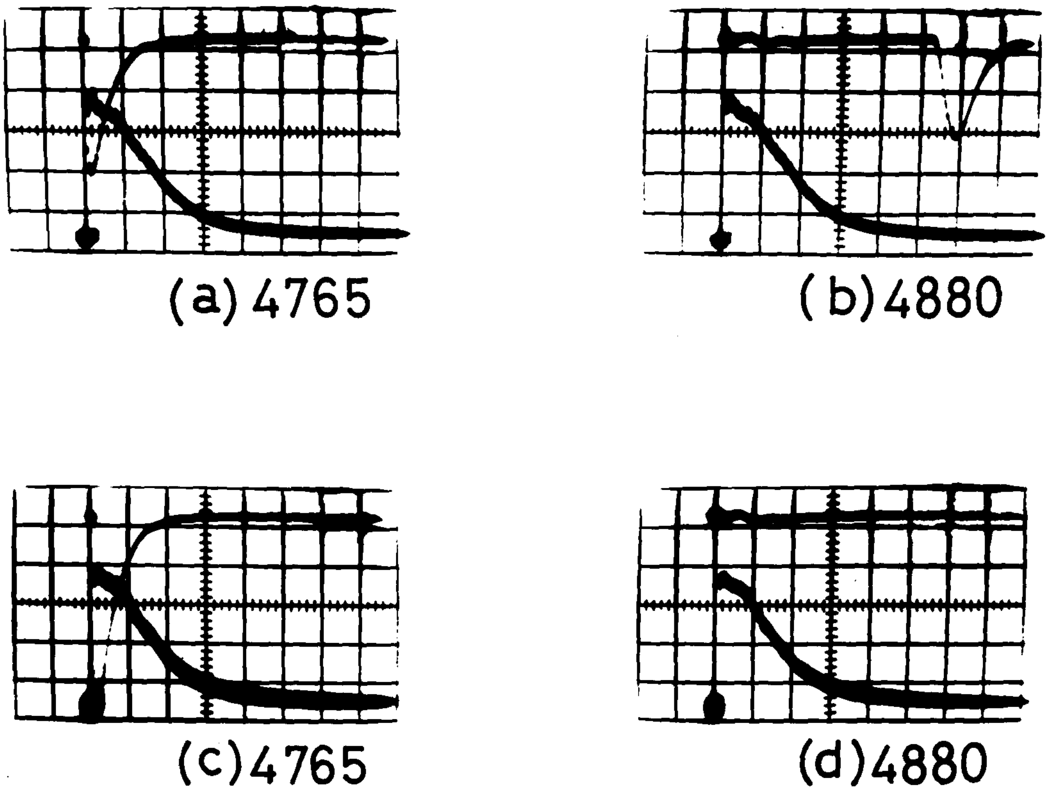

Fig.8

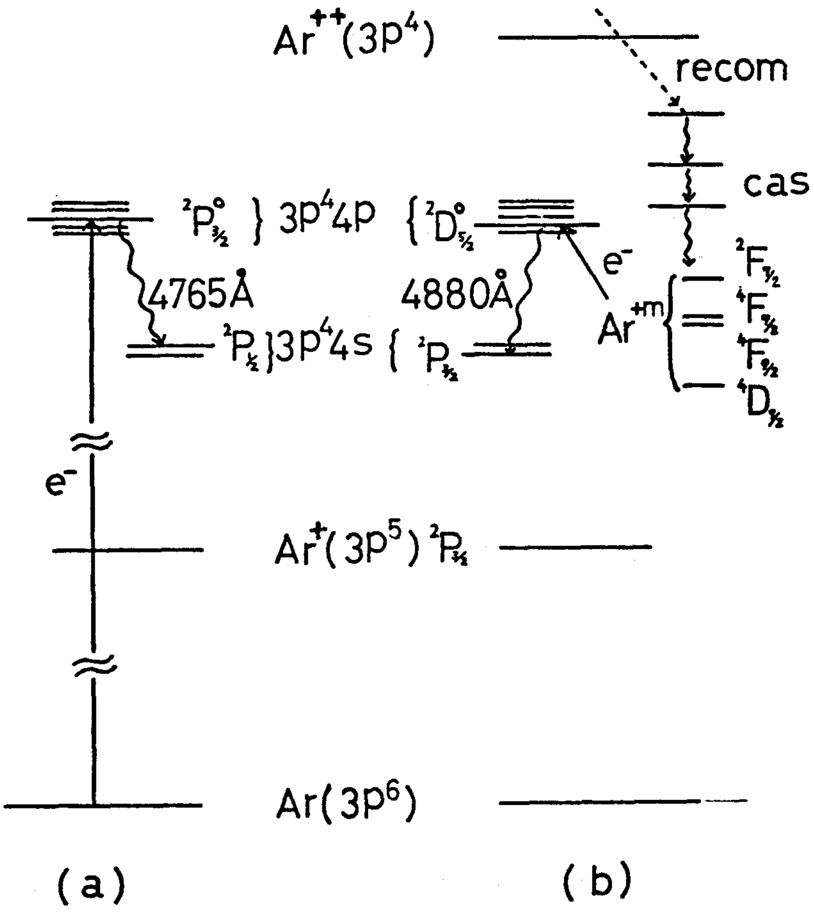
Ar^{++}(3P^4)
recom
cas
$^2P^o_{3/2}$ } 3P^{4}4P {$^2D^o_{5/2}$
4765Å
4880Å
e$^-$
$^2F_{7/2}$
$^4F_{5/2}$
$^4F_{9/2}$
$^4D_{7/2}$
Ar^{+m}
$^2P_{1/2}$}3P^{4}4s { $^2P_{3/2}$
e$^-$
Ar$^+$(3P^5) $^2P_{3/2}$
Ar(3P^6)
(a)
(b)

Fig.9

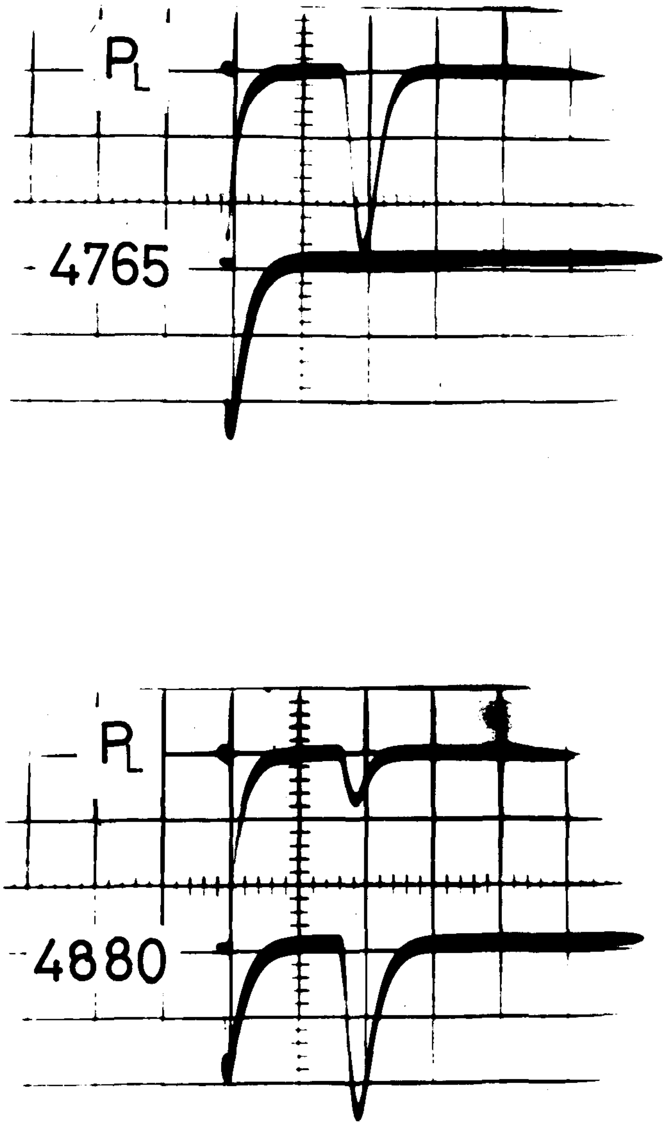

Fig.10

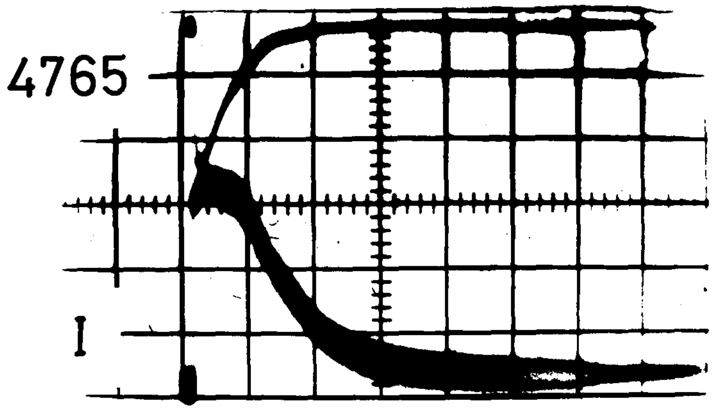

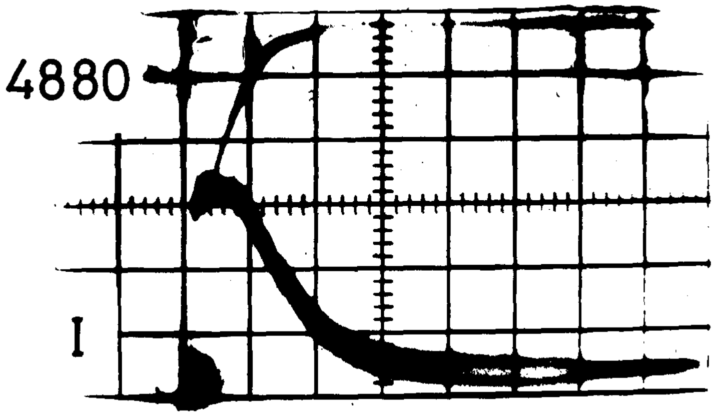

Fig.11

2. On the Correlation between Laser Action and Linear Pinch

(1) Introduction

Recently, argon ion laser actions have been realized in such a plasma as produced by a linear pinch discharge and time correlations between laser actions and linear pinch have been reported by several workers.[1~5]

The present experiments are also carried out in a linear pinch discharge through argon. However, the period of the discharge current is about 30 μsec, and much longer than that reported by others. Laser actions take place only at the beginning of the discharge. In addition, little correlation between laser actions and pinch can be recognized in this study.

(2) Experimental procedures

Two discharge tubes made of Pyrex glass and fitted with Brewster quartz windows are used in the present experiments. One is 20 mm in diameter, and 100 cm in length. The other is 40 mm in diameter, and 100 cm in length. In addition, two pairs of laser mirrors are used. For visible laser lines, a pair of dielectric-coated spherical mirrors are used. Their radii of curvature are both 150 cm. For ultraviolet laser lines, an aluminum-coated plane mirror and an aluminum-coated spherical mirror whose radius of curvature is 400 cm are used.

Condensed discharges through argon take place between a pair of cold aluminum ring electrodes separated by a distance of 100 cm. One of the electrodes is connected to a condenser bank through an air gap switch, and the other is grounded through six copper belts which surround the tube concentrically and serve as return circuits, as shown in Fig.1. The tube is evacuated by an oil diffusion pump down to about 1×10^{-5} torr and then argon gas is admitted. Condensed discharges through argon are powered by 2, 4, and 50 μF capacitor banks charged up to 18 kV. When a 50 μF capacitor is used, no laser action is obtained. Intense laser actions occur with a 2 μF capacitor bank charged up to 15 kV.

Quick change of the voltage between the electrodes is recorded in the conventional way through a 200:1 voltage divider. Variation of the discharge current is observed by use of a Rogowski coil.

The pinch of the plasma is observed by use of a camera with a neutral density filter. The light beam coming through the low reflectivity mirror is led onto the ground glass plate set on the path of the beam and the pattern projected there is recorded with another camera at the same time. In addition, the light beam is in part led into an entrance slit of a monochromator. Variations in intensity of the laser lines are observed with a photomultiplier of RCA 1P28, which is connected directly to a dual beam cathode ray oscilloscope. Change in intensity of the spontaneous emission radiated outside the tube is traced by use of another phototube and the oscilloscope.

(3) Experimental results

The time integrated laser spectra obtained with the 40 mmΦ tube are presented in Fig.2(a) to (c), as a function of the applied voltage. At the applied voltage of 15 kV and the pressure of 13 mtorr, all the six laser lines exhibit themselves at 4579, 4765, 4880, 4965, 5017, and 5145 Å as shown in Fig.2(b). When the 20 mmΦ tube with aluminum-coated mirrors is operated under the same discharge conditions as above, only two laser lines 4765 and 3511 are observed as shown in Fig.2(d). For comparison, a typical spontaneous emission spectrum obtained directly from the discharge tube without the mirrors is shown in Fig.2(e).

The transitions for the laser lines observed and the term symbols for the levels concerned are shown in Fig.3 on the basis of the tabulated energy levels presented by Moore.[6)]

In Fig.4, the time resolved behaviour of the lines 4765 and 4880 are shown in relation to the spontaneous emission P_s, the discharge voltage V, and the discharge current I.

The pinch and the projected pattern, which are simultaneously obtained with the use of the 40 mmϕ tube, are presented in Fig.5, as a function of the initial filling pressure. At the left side of the figure, one can see whether the pinch effect is realized or not. Each of the photos shows a time integral of the flash emission during single discharge. The line of sight into the discharge chamber is perpendicular to the axis of the tube. Two dotted lines show the wall of the tube. At higher pressures than 16 mtorr, the projected patterns are nearly the same among them as typically shown at the right side of the figure. On the other hand, the pattern obtained at the pressure of 13 mtorr is quite different from that obtained above 16 mtorr. Judging from the fact that the colour of the latter pattern is blue-green, laser actions do take place only at the pressure corresponding to (e).

When the 20 mmϕ tube with the aluminum-coated mirrors is used, laser actions for the lines 4765 and 3511 take place at the pressure under which the pinch cannot be clearly seen. In other words, whenever the narrow bright pinch is clearly seen along the axis of the tube, laser actions do not occur.

(4) Discussions

Laser actions take place only at the beginning of the discharge in spite of its long period. In the previous chapter, where a 5 mmϕ tube was used, the laser action for the line 4880 took place in two different moments, one at the early stage and the other in the afterglow of the discharge. The failure in appearance of the secondary pulse in the present experiment may be attributed to the impurity effect. In fact, it is inevitable that impurity species are present in a plasma produced by such a violent condensed discharge.

There has been a hypothesis proposed by Bennett that combines laser output with pinch effect.[7)] To put it briefly, the strong field produced by magnetohydrodynamic instabilities accompanied by the pinch can accelerate electrons to the high energies of importance in the sudden perturbation process. And the field also accelerates the ions in the system and can reduce the problem of the resonance radiation trapping by producing extremely Doppler broadening of the pertinent resonance transitions to the ion ground state. The present observation, however, shows that there are no correlations between laser actions and pinch phenomena, as long as the periods of the discharge currents are about 30 μsec.

On the other hand, there have previously been several reports concerning the correlation between the appearance time of the laser pulse and the pinch time.[1~5] Some of the characteristics of the typical laser devices are compared with each other in Table 1. The discharge conditions are not so varied, while the period of the discharge current, T, in the present device is much longer than others. It may be due to a larger condenser bank and an increase in the self-inductance of the discharge circuit.[8]

By the way, the period of the discharge current may have close relation to the pinch time. Two contraction mechanisms have been confirmed in the plasma produced by linear pinch discharges according to the initial filling pressures.[9] One of them is the so-called "snowplow model" and this model can be applied at relatively lower pressures. The other is the so-called "shock wave model". At such low pressures as the laser actions can take place, the former model may be applied. According to this model, the pinch time, τ_p, is calculated numerically by the following equation,[10] and is also presented in the table,

$$\tau_p = 1.43 \cdot R \cdot \left[\frac{4\Pi^2 \rho}{\mu_0 C^2 V^2 W^4} \right]^{1/4} \quad ,$$

where R is the inner diameter of the tube, ρ the density of the argon in the tube, μ_0 the magnetic permeability, C the capacitor of the bank, V the discharge voltage, and W the angular frequency of the discharge current (=2Π/T). It would take about 4 μsec for the plasma under the present discharge condition to contract itself. The actual plasma, however, does not contract itself, and accordingly they are indicated by the mark "X" in Table 1.

The mark "*" in the last column means that the appearance time of the laser pulse, τ_l, and the pinch time observed, τ_o, have been obtained from different shots of the discharge. The mark "?" means that it is obscure whether τ_l and τ_o have been observed simultaneously or not.

Although the pinch time can be calculated in this way, it is another problem whether the plasma contracts itself or not. That is, even if the pinch time calculated coincides with the appearance time of the laser pulse, it cannot be said that correlations between laser actions and pinch are established. Violent condensed discharges are generally poor in reproducibility to be exact. Accordingly, it may be most desirable to observe the laser pulse and pinch phenomena simultaneously. In addition, even if the pinch time observed happens to agree with the appearance time of the laser pulse in such a rapid contraction of the discharge, it seems to be a debatable question from the accurate point of view that there are correlations between them. Accordingly, it may be desirable to observe the correlations under the condition that the contraction of the plasma produced is as slowly as possible.

References

1) S.G.Kulagin, V.M.Likhachev, E.V.Markuzon, M.S.Rabinovich and V.M.Sutovskii : Soviet Phys. JETP Letters 3 (1966) 6.

2) V.M.Likhachev, M.S.Rabinovich and V.M.Sutovskii : Soviet Phys. JETP Letters 5 (1967) 43.

3) A.N.Vasileva, V.M.Likhachev and V.M.Sutovskii : Soviet Phys. Tech. Phys. 14 (1969) 246.

4) R.Illingworth : J. Phys. D ; Appl. Phys. 3 (1970) 924.

5) Y.Hashino, Y.Katsuyama and K.Fukuda : Japan. J. appl. Phys. 11 (1972) 907.

6) C.E.Moore : Atomic Energy Levels, Vol.1 (National Bureau of Standards, Washington, D.C., 1949)

7) W.R.Bennett,Jr. : Chemical Lasers, Appl. Optics Suppl. 2 (1965) p.3.

8) T.Iwai, M.Ishigami, J.Yoda, H.Kumazawa and T.Horie : Japan. J. appl. Phys. 9 (1970) 516.

9) K.Ishii, H.Suemitsu and K.Fukuda : Japan. J. appl. Phys. 5 (1966) 1235.

10) O.A.Anderson, W.R.Baker, S.A.Colgate, J.Ise,Jr. and R.V.Pyle : Phys. Rev. 110 (1958) 1375.

Figure Captions

Fig.1 A schematic view of the 40 mmϕ laser tube.
T,trigger; C,capacitor bank.

Fig.2 Argon ion laser spectra (a) to (d) and spontaneous emission spectrum (e), at the pressure of 13 mtorr.
(a) 12kV, 40mmϕ tube. (b) 15kV, 40mmϕ tube. (c) 18kV, 40mmϕ tube. (d) 15kV, 20mmϕ tube with aluminum-coated mirrors.
(e) typical spontaneous emission spectrum, 10kV, 23mtorr, 20mmϕ tube without mirrors.

Fig.3 The energy level diagram for the observed argon ion laser transitions.

Fig.4 Time resolved behaviour of the laser lines 4765 (left) and 4880 (right), in comparison with the spontaneous emission P_s, the waveforms of the discharge voltage V, and the discharge current I.
(a) 20mmϕ tube, 2μsec/div. (b) 40mmϕ tube, 20μsec/div.
(c) 40mmϕ tube, 10μsec/div.

Fig.5 Dependence of the pinch and the projected pattern upon the initial filling pressure at 15kV.
(a) 43mtorr. (b) 23mtorr. (c) 18mtorr. (d) 16mtorr.
(e) 13mtorr.

Table 1 Characteristics of the laser actions in the linear pinch discharge.

V, discharge voltage; R, inner diameter of the tube; C, capacitor of the bank; T, period of the discharge current; P, optimum pressure for the laser actions; L, laser lines; τ_l, appearance time of the laser pulse; τ_p, pinch time calculated; τ_o, pinch time observed.

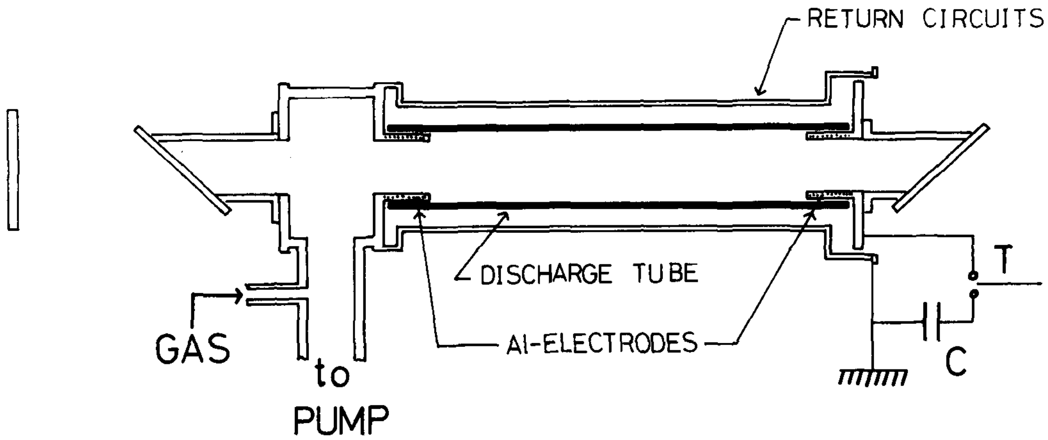
RETURN CIRCUITS
DISCHARGE TUBE
T
GAS
to
PUMP
Al-ELECTRODES
C

Fig.1

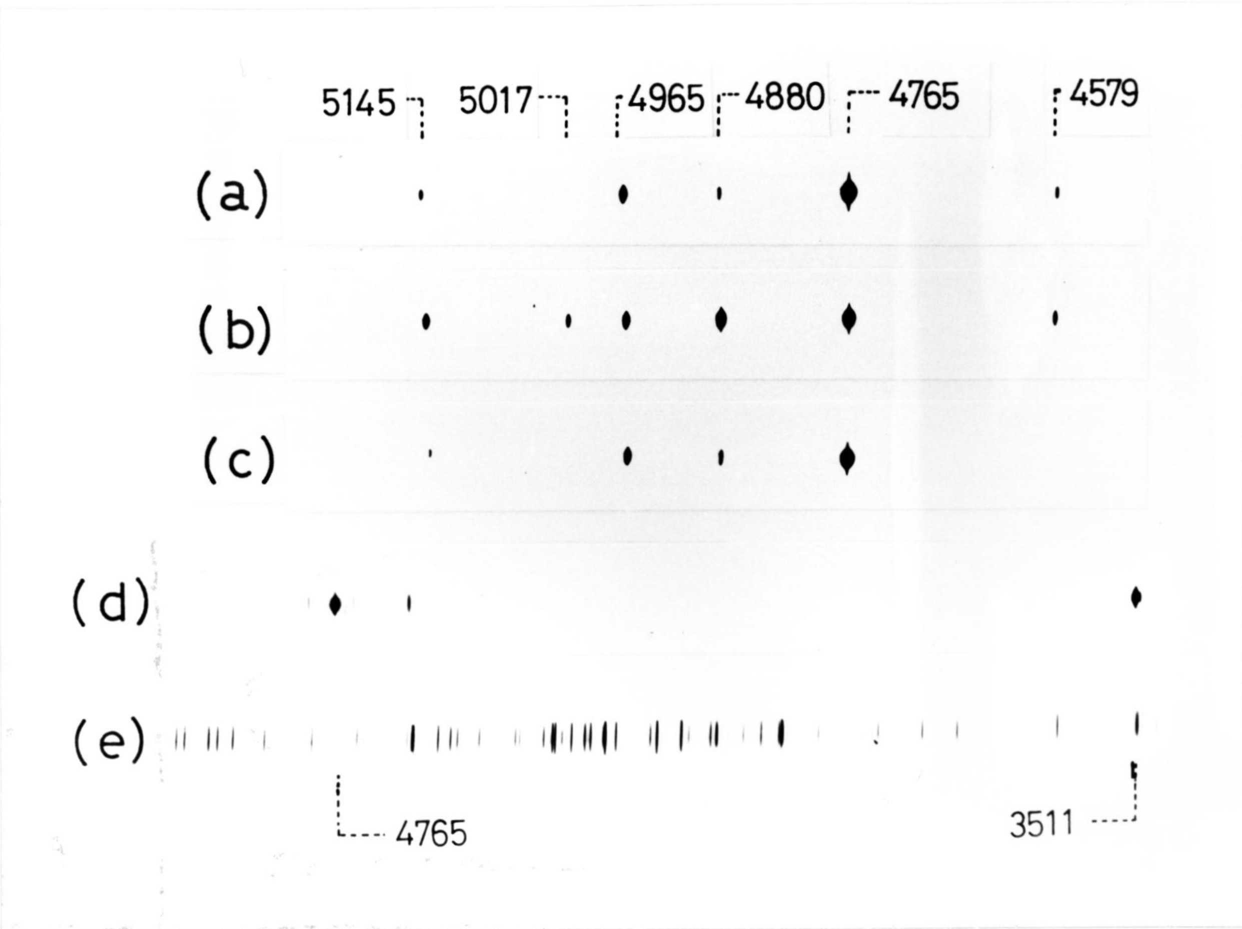

Fig.2

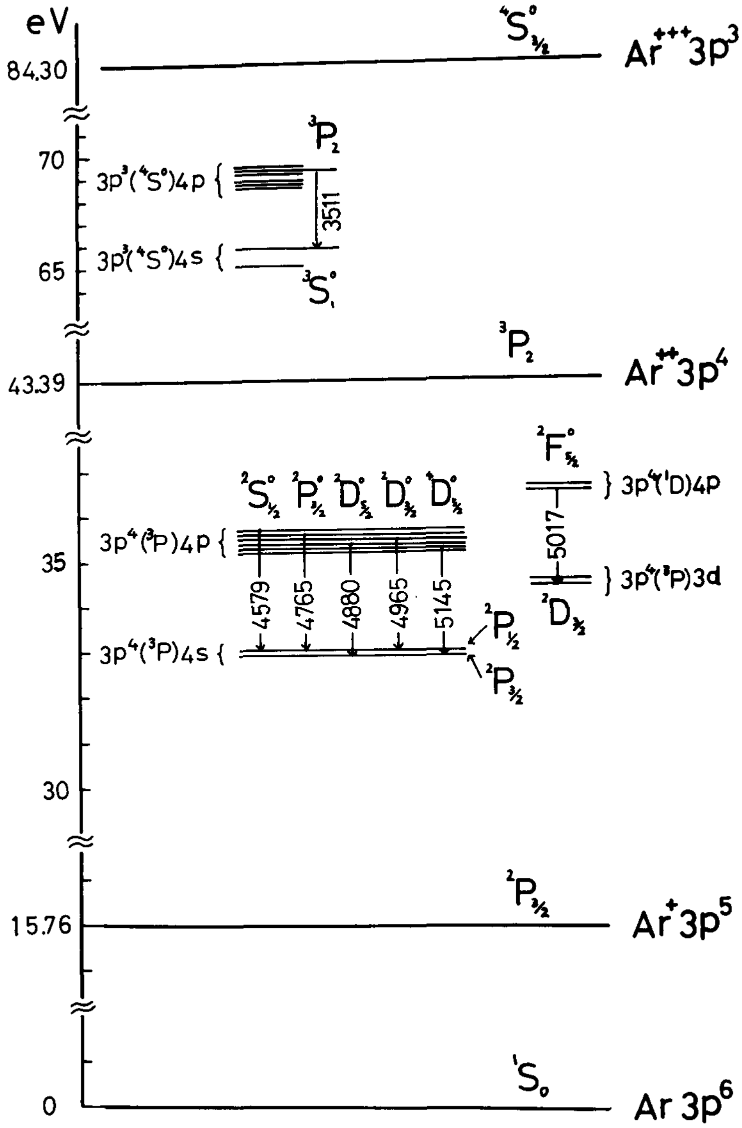
eV
84.30
70
65
43.39
35
30
15.76
0
$^4S^\circ_{3/2}$
$Ar^{+++}3p^3$
$^3P_2$
$3p^3(^4S^\circ)4p$
3511
$3p^3(^4S^\circ)4s$
$^3S^\circ_1$
$^3P_2$
$Ar^{++}3p^4$
$^2F^\circ_{5/2}$
$3p^4(^1D)4p$
5017
$3p^4(^3P)3d$
$^2D_{3/2}$
$^2S^\circ_{1/2}$ $^2P^\circ_{3/2}$ $^2D^\circ_{5/2}$ $^2D^\circ_{3/2}$ $^4D^\circ_{5/2}$
$3p^4(^3P)4p$
4579
4765
4880
4965
5145
$3p^4(^3P)4s$
$^2P_{1/2}$
$^2P_{3/2}$
$^2P_{3/2}$
Ar^+3p^5
$^1S_0$
$Ar\ 3p^6$

Fig.3

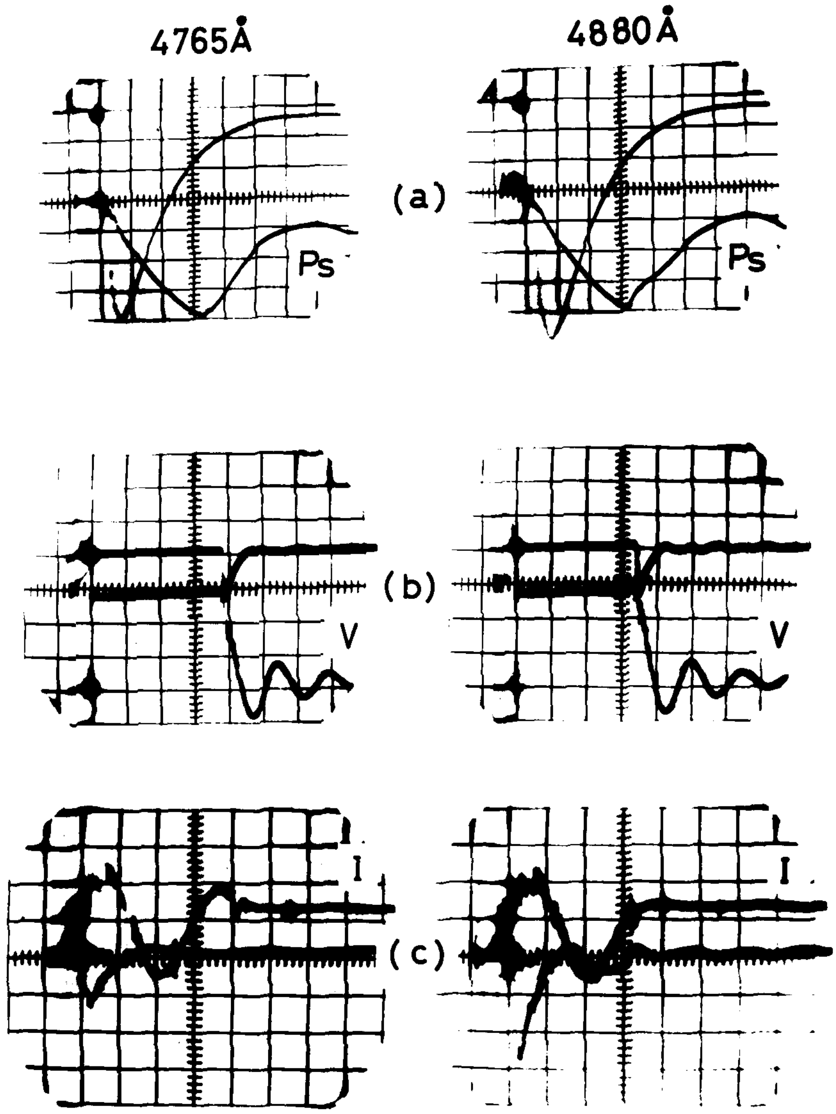

Fig.4

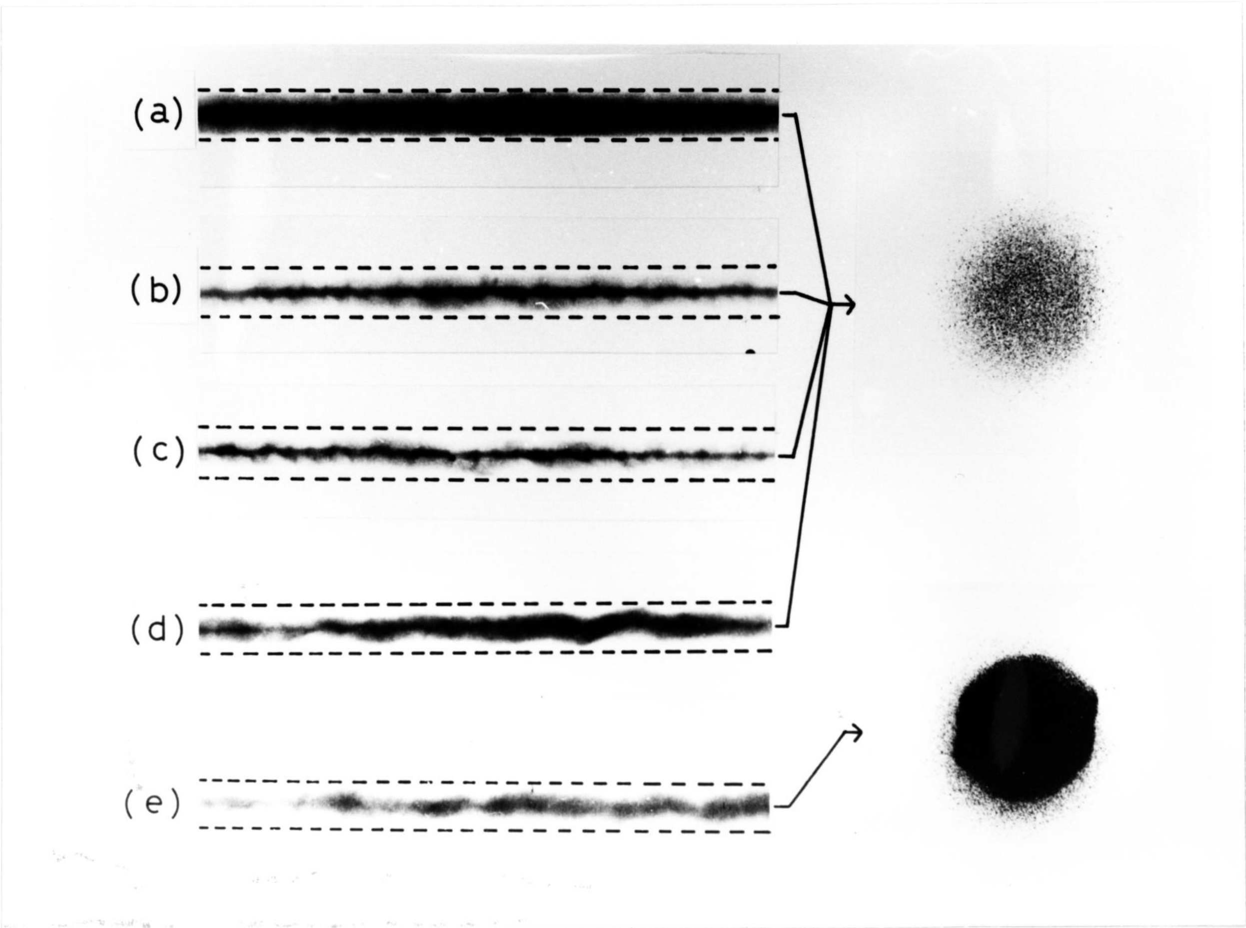

Fig.5

TABLE 1

	V kV	R mm	C μF	T μsec	P mtorr	L Å	τ_l μsec	τ_p μsec	τ_0 μsec
KULAGIN. et al.[1]	25	25	0.4	1.6	12	4765	0.3	0.25	
LIKHACHEV. et al[2]	45	40	0.4	2	1		0.5	0.2	0.5*
VASILEVA.et al[3]	25	20	0.4	3	14	4765 3511	0.2 0.4	0.4	0.4?
ILLINGWORTH[4]	17	52	2	2.4	5 20	4765 3511	0.4 0.7	0.3 0.5	× 0.6*
HASHINO.et al.[5]	30	20	1	7	10	4765 3511	0.2 0.3	0.5	
KODA. et al.	18	40	2	30	13 14	4765 3511	1.3	4.0 4.1	× ×

Acknowledgements

The author would like to express his hearty gratitude to his thesis advisor, Professor Tadao HORIE for his valuable advice and continual encouragement in all phases of the present work. He would like to thank Associate Professor Tsuruji IWAI for his helpful advice and invaluable suggestion. He would like to express his thanks to Professor Yoshiaki NAKASHIMA of Wakayama University for his help in designing and constructing the laser apparatus and for his helpful discussions. He wishes to thank Associate Professor Yoichi WATANABE of College of General Education, Osaka University, for his theoretical suggestion of the shock wave.
He is much indebted to the members of the laboratory for their encouragements and assistances, and to the members working in the Central Workshop of Osaka University on the Toyonaka Campus for their excellent technical aids.